



OPEN ACCESS

EDITED BY

Dezhong Zhou,
Xi'an Jiaotong University, China

REVIEWED BY

Dana Akilbekova,
Nazarbayev University, Kazakhstan
Francesco Bairo,
Polytechnic University of Turin, Italy

*CORRESPONDENCE

Morteza Alizadeh,
✉ mor1361@gmail.com

RECEIVED 17 February 2023

ACCEPTED 05 June 2023

PUBLISHED 19 June 2023

CITATION

Gharibshahian M, Salehi M,
Beheshtizadeh N,
Kamalabadi-Farahani M, Atashi A,
Nourbakhsh M-S and Alizadeh M (2023),
Recent advances on 3D-printed PCL-
based composite scaffolds for bone
tissue engineering.
Front. Bioeng. Biotechnol. 11:1168504.
doi: 10.3389/fbioe.2023.1168504

COPYRIGHT

© 2023 Gharibshahian, Salehi,
Beheshtizadeh, Kamalabadi-Farahani,
Atashi, Nourbakhsh and Alizadeh. This is
an open-access article distributed under
the terms of the [Creative Commons
Attribution License \(CC BY\)](https://creativecommons.org/licenses/by/4.0/). The use,
distribution or reproduction in other
forums is permitted, provided the original
author(s) and the copyright owner(s) are
credited and that the original publication
in this journal is cited, in accordance with
accepted academic practice. No use,
distribution or reproduction is permitted
which does not comply with these terms.

Recent advances on 3D-printed PCL-based composite scaffolds for bone tissue engineering

Maliheh Gharibshahian¹, Majid Salehi^{2,3}, Nima Beheshtizadeh^{4,5},
Mohammad Kamalabadi-Farahani², Amir Atashi³,
Mohammad-Sadegh Nourbakhsh⁶ and Morteza Alizadeh^{2*}

¹Student Research Committee, School of Medicine, Shahroud University of Medical Sciences, Shahroud, Iran, ²Department of Tissue Engineering, School of Medicine, Shahroud University of Medical Sciences, Shahroud, Iran, ³Tissue Engineering and Stem Cells Research Center, Shahroud University of Medical Sciences, Shahroud, Iran, ⁴Regenerative Medicine Group (REMEDI), Universal Scientific Education and Research Network (USERN), Tehran, Iran, ⁵Department of Tissue Engineering, School of Advanced Technologies in Medicine, Tehran University of Medical Sciences, Tehran, Iran, ⁶Faculty of New Sciences and Technologies, Semnan University, Semnan, Iran

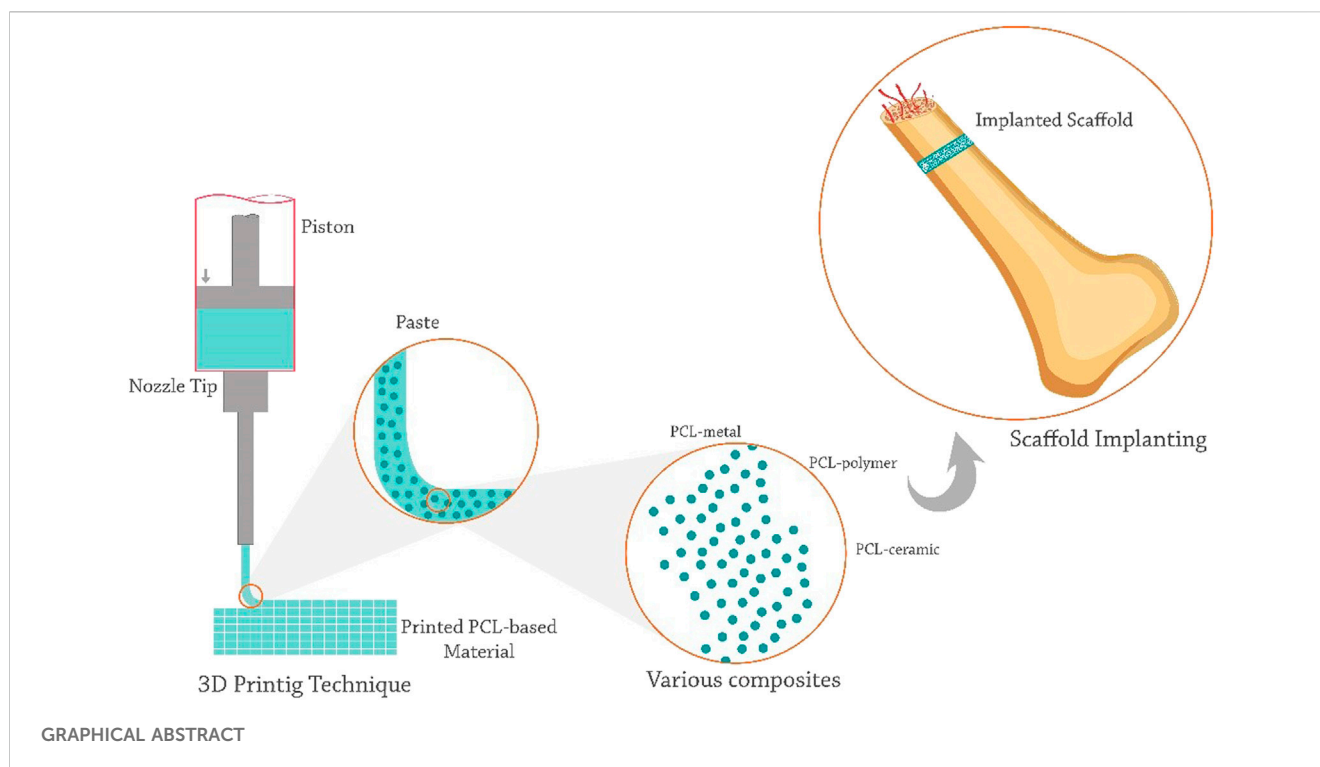
Population ageing and various diseases have increased the demand for bone grafts in recent decades. Bone tissue engineering (BTE) using a three-dimensional (3D) scaffold helps to create a suitable microenvironment for cell proliferation and regeneration of damaged tissues or organs. The 3D printing technique is a beneficial tool in BTE scaffold fabrication with appropriate features such as spatial control of microarchitecture and scaffold composition, high efficiency, and high precision. Various biomaterials could be used in BTE applications. PCL, as a thermoplastic and linear aliphatic polyester, is one of the most widely used polymers in bone scaffold fabrication. High biocompatibility, low cost, easy processing, non-carcinogenicity, low immunogenicity, and a slow degradation rate make this semi-crystalline polymer suitable for use in load-bearing bones. Combining PCL with other biomaterials, drugs, growth factors, and cells has improved its properties and helped heal bone lesions. The integration of PCL composites with the new 3D printing method has made it a promising approach for the effective treatment of bone injuries. The purpose of this review is give a comprehensive overview of the role of printed PCL composite scaffolds in bone repair and the path ahead to enter the clinic. This study will investigate the types of 3D printing methods for making PCL composites and the optimal compounds for making PCL composites to accelerate bone healing.

KEYWORDS

bone tissue engineering, PCL composites, 3D printing, bone scaffolds, 3D printed PCL

1 Introduction

Bone is a specialised connective tissue composed of a calcified extracellular matrix (ECM) and three main types of cells: osteocytes, osteoblasts, and osteoclasts (Rho et al., 1998). Bone tissue plays multiple roles in daily life, including storing and releasing minerals, supporting the body, enabling and facilitating movement, and



protecting the body's internal organs (L Mescher, 2018). Many people suffer from bone diseases caused by tumour resection, trauma, infection, cysts, congenital defects, and injuries caused by accidents (Li et al., 2020a; Biscaia et al., 2022a). Bones are dynamic and vascular organs that are regenerated and repaired throughout (Heo et al., 2017; Hassanajili et al., 2019a). Bone fracture repair occurs during the four phases of hematoma formation, soft callus formation, hard callus formation, and bone remodelling (Monfared et al., 2022).

Bone tissue has a strong potential to regenerate itself after injury; however, effective repair of large and critical bone defects still requires bone grafts (Carano and Filvaroff, 2003; Lanza et al., 2020). More than two million bone graft surgeries are performed each year, more than a quarter of which are performed in the United States (Campana et al., 2014; Buyuksungur et al., 2021a). Demand for bone grafts is expected to increase in the coming decades as the population ages (for example, in Germany, half of the population is over 45 and one-fifth is over 66) (Huber et al., 2022). Natural bone replacements have been widely used in clinical applications. Autograft is the most commonly used traditional option for patients with osteoporosis; however, complex issues such as donor site complications, infection risk, and a lack of bone grafts of appropriate size and shape have limited its use in orthopaedic applications (Keating et al., 2005; Rezanian et al., 2022a). In addition, allograft will be a treatment option that uses a bone replacement from another person. Transmission of infection and disease, limited resources, insufficient integration with bone tissue, and the risk of immune rejection are also obstacles to the success of allografts (Fleming et al., 2000; Erbe et al., 2001).

Bone tissue engineering (BTE) is one of the best alternative methods to overcome these shortcomings, as it can be produced on a large scale without immune rejection (Hwang K.-S. et al., 2017). BTE focuses on key processes such as cell growth, customization of bone grafts, and minimization of the need for additional surgeries (Kim S. E. et al., 2016; Hwang K.-S. et al., 2017). It uses a three-dimensional (3D) scaffold to create the proper microenvironment for cell proliferation and regeneration of damaged tissues or organs (Biscaia et al., 2022a). In BTE, biomaterials are used alone or in combination with appropriate biological, chemical, and mineral agents to repair damaged bone tissue (Hernandez et al., 2017a).

An efficient 3D scaffold for BTE must possess unique features such as osteoinduction, osteoconduction, and osseointegration (Beheshtizadeh et al., 2021; Duan et al., 2021). Osteoconductivity of the scaffold helps eliminate the formation of fibrous capsules and creates a strong bond with the host bone (Wang C. et al., 2017; Zimmerling et al., 2021). These biomimetic scaffolds should possess biocompatibility and bioactivity to encourage appropriate cellular adhesion. Furthermore, these scaffolds should replicate bone structure, shape, and function (Park H. et al., 2018; Koons et al., 2020).

Scaffolds must also have optimal geometry and porosity, which are critical to preserving space for bone regeneration, supporting the periosteum, and filling the anatomical structure of bone defects (Ku et al., 2015; Giuliani et al., 2016; Koons et al., 2020). The interconnected shape of macro- and microporosity allows bone tissues and arteries to grow inside the scaffold and deliver nutrients and oxygen to the cells. Different pore sizes affect cell behavior, and pore sizes close to 300 μm are optimal for bone growth (Karageorgiou and Kaplan, 2005; Rezwan et al., 2006). Additionally,

the scaffold needs to be mechanically strong enough to support the structural requirements of the tissue replacement, and its gradual degradation rate must be proportional with growth, cell proliferation, and new bone tissue formation. The scaffold must have an elastic modulus similar to human bone tissue (7 GPa–25 GPa) to prevent stress shielding (Pattanashetti et al., 2019; Fallah et al., 2022; Huber et al., 2022).

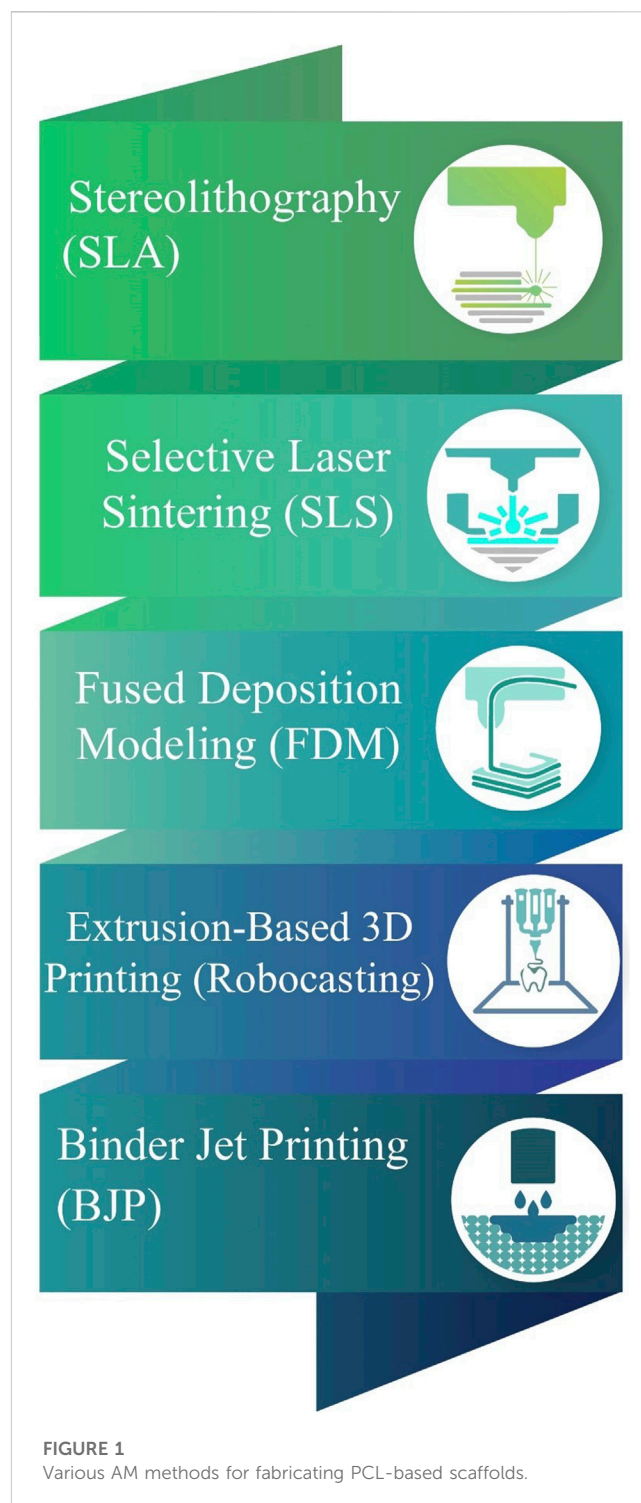
The used materials and the scaffold's fabrication methods are key parameters in controlling its properties. Various traditional methods such as, solvent casting (Thadavirul et al., 2014), electrospinning (Metwally et al., 2020), and phase separation (Salerno and Domingo, 2015) have been used in the BTE approach. Since traditional techniques cannot precisely control the size, geometry, and interconnection of scaffold pores, in recent years, additive manufacturing methods [e.g., 3D printing (Liu Y. et al., 2020; Zimmerling et al., 2021)] have been considered as a promising approach to repairing critical bone defects in a clinical setting (Sachlos and Czernuszka, 2003; Wubneh et al., 2018).

A 3D printing technique possessing appropriate features, such as spatial control of micro-architectural and scaffold composition and high efficiency and accuracy, has become one of the top research topics in BTE (Galarraga et al., 2019; Wang et al., 2020; Wang F. et al., 2022; Wang P. et al., 2022). This technique has revolutionised scaffold fabrication and is generally regarded as the most symbolic tool of the third industrial revolution (Wibowo et al., 2020; Xu Z. et al., 2021).

Due to the diversity of the molecular weight, surface chemistry, and crystallinity of various biomaterials, the scaffold's swelling, biocompatibility, degradability, and mechanical properties are varied (Burg et al., 2000; Rezwan et al., 2006). Therefore, choosing a suitable biomaterial is also quite essential. Various polymeric (Grémare et al., 2018), metal (Ahn et al., 2018), ceramic (Mondal et al., 2020), and composite (Farokhi et al., 2018) materials have been used to fabricate bone scaffolds. PCL is one of the most common materials in bone tissue regeneration (Wang C. et al., 2022). The slow degradation of PCL provides adequate time for bone regeneration and can also be manipulated to regulate the biodegradability rate of this polymer. Studies showed that PCL is completely degraded *in vivo* within 3–4 years after transplantation and has excellent bone graft stability and affinity (Xue et al., 2017; Gautam et al., 2021).

However, due to the hydrophobicity and lack of osteogenesis potential of PCL, researchers generally use PCL-based composite scaffolds [in combination with a variety of metal (Wang S. et al., 2022; Lei et al., 2022), polymer (Ke et al., 2022), and ceramic (Cao et al., 2022) materials] for tissue engineering applications to improve the mechanical and biological properties of the prepared constructs (Chen et al., 2004; Xiao et al., 2021).

This study highlights the opportunities and challenges of PCL-based 3D printed composite scaffolds for BTE and identifies the path ahead for them to enter the clinic. First, it introduces the types of 3D printing methods that have been used so far for PCL-based composite scaffolds for BTE and describes the parameters affecting the optimal design of the relevant inks. Then, it



introduces the types of ceramic, polymer, and metal materials that have been used in combination with PCL and 3D printing for BTE. The later sections express the importance of the presence of drugs, growth factors, and cells in the above composites for bone repair. Finally, the clinical trials and the future path of these scaffolds to enter the clinic will be discussed.

2 Additive manufacturing techniques

The additive manufacturing (AM) technology mainly includes fused deposition modelling (FDM), binder jetting, directional energy deposition, material extrusion, selective laser sintering (SLS), material jetting, Sheet Lamination, Vat Photopolymerization, Powder Bed Fusion, and stereolithography (SLA) (Murphy and Atala, 2014; Turnbull et al., 2018; ASM International et al., 2020). AM produces objects through the successive layering of powders, liquid, or solid materials in accordance with a 3D design and the specified process parameters. The AM technology makes it possible to control the temporal and spatial distribution of inks (cells and biomaterials) and the spatial distance between them. Patient-specific computer-aided design (CAD) models can be created by converting computed tomography (CT) or magnetic resonance imaging (MRI) images of clinical defects to CAD models. Other facilities are then used to cut CAD models into G-code, which encrypts 3D CAD models into a format that can control the machine (Boschetto and Bottini, 2014; Mohamed et al., 2015; Zimmerling et al., 2021). Reproducibility, precise deposition, the creation of complex high-resolution 3D structures, cost-effectiveness, controlled morphology and size of pores, simplicity, and the ability to control cell distribution are just some of the advantages of AM methods (Haffner et al., 2018; El-Habashy et al., 2021).

The AM techniques allow the integration of vascular structures in tissue engineering constructs and thus overcome the challenges of nutrient transfer in scaffolds made with other methods (Hann et al., 2019). This approach seeks to develop innovative scaffolds that enhance the mechanical properties of BTE constructs in load-bearing applications (Farzadi et al., 2014; Wang L. et al., 2017). The AM increases the efficiency of tissue engineering scaffolds by using a wide range of materials and cells within the final structure. To achieve this, the biomaterials must possess a high rate of printability (Kyle et al., 2017; Zimmerling et al., 2021). The constructs obtained by AM facilities can be mixed with live cells before fabrication (in some techniques) or loaded with cells upon fabrication. A printed material may require post-processing procedures such as the removal of preservatives, surface modification, and sintering in order to

mature and achieve the desired geometry and structure (Temple et al., 2014; Haffner et al., 2018).

The AM methods can adjust various properties of bone scaffolds, such as stiffness, the spatial distribution potential of biochemical factors, complex and irregular shapes, pore shapes and dimensions, and surface morphology (Cox et al., 2015; Wang et al., 2016a; Du et al., 2019). In addition, this technology allows for high cell density and *in vivo* interaction. Ink containing various cell types and ECMs can print large-scale damaged bone scaffolds through the high-density bioprinting techniques (Rusmueller et al., 2015; Celikkin et al., 2022). The possibility of processing drugs and biomolecules using various materials, maintaining structure and shape, minimising material loss, improving mechanical properties, and increasing cell penetration and nutrient circulation have made the AM a desirable approach in BTE (Chen et al., 2020; Celikkin et al., 2022). A variety of materials could be used in AM strategies, including natural and synthetic materials. Meanwhile, PCL, a printable thermoplastic polymer (melting point 59°C–64°C), is one of the first polymers used in this technique. For the first time in 2006, 3D-printed PCL scaffolds were able to receive FDA approval as a bone filler in skull and facial applications (FDA, 2006).

2.1 Various AM techniques used for PCL-based scaffold fabrication

The properties of the 3D printing scaffold are affected by the printing technology. AM techniques used in fabricating the PCL-based scaffolds include SLA (Elomaa et al., 2020), SLS (Eosoly et al., 2012), FDM (Bruyas et al., 2018a), and bioprinting (Koch et al., 2022) (Figure 1). These methods were summarized in Table 1.

FDM, or fused filament fabrication (FFF), is the preferred method for PCL deposition. PCL's thermoplasticity has made it a desirable polymer for the available and uncomplicated FDM method (Arealis and Nikolaou, 2015; Xu X. et al., 2021). PCL filaments or small grains begin to melt by being placed in a temperature-controlled printing head, melt extrude of a small nozzle, and are layered on a platform to build a 3D structure (Xu et al., 2014; Arealis and Nikolaou, 2015). In the printing environment, the melt gradually cools and creates a scaffold with high reproducibility and controlled pores (Schantz et al.,

TABLE 1 3D printing methods for PCL-based scaffolds.

AM technique	Advantages	Disadvantages	Ref
FDM	Appropriate mechanical and biochemical properties for bone regeneration; available, user-friendly, reproducible	High temperature, limited resolution	Zhao et al. (2020a), Xu et al. (2021b)
SLS	Control pore size and porosity, non-load-bearing scaffolds	Expensive, high temperature, not able to create small pores	Partee et al. (2006), Liu et al. (2020b)
SLA	High accuracy, produce complex shapes, high resolution	Expensive, difficult to build micron-sized scaffolds, limited layer thickness, cytotoxicity caused by photoinitiator	Melchels et al. (2010), Elomaa et al. (2011a), Elomaa et al. (2020)
Binder-jet-based	Cheap, fast, cell survival rate of 85%, Compatible with various materials	Limited direction of injection, low resolution, low cell density	He, 2016; He et al. (2017)
Extrusion-based	Simple, inexpensive, cell survival rate of 40%–80%, tunable speed, high cell density	Slow, limited material	Pati et al. (2015a), Borkar et al. (2021)

2005). However, the high temperature of this method has limited the use of heat-sensitive biomolecules and polymers in combination with PCL.

In this method, the viscosity of the melted polymer restricts the resolution, shape, and even regularity of the scaffold (Zein et al., 2002; Zhao et al., 2020a). The PCL scaffolds obtained by this method have dimensions of hundreds microns (sometimes up to millimeters) (Xie et al., 2019). Zhao et al. (Zhao et al., 2020a) used the FDM method to print magnesium/PCL composite scaffolds. Their results showed that the resulting scaffold had suitable biocompatibility, mechanical properties, and osteogenesis. Using this method, they were able to evenly mix and print the optimal percentage of magnesium inside the scaffold. Rezania et al. (Rezania et al., 2022a) used this method to print hydroxyapatite/PCL scaffolds. Hydroxyapatite/PCL filaments showed that this method could be considered a commercially viable and suitable method for producing scaffolds with appropriate mechanical and biological properties for BTE applications.

SLS is a more expensive but more accurate method for fabricating PCL composite scaffolds. The SLS equipment has several parts, including a laser source, a powder bed, and a piston and roller to spread a new layer of powder (Williams et al., 2005; Partee et al., 2006). The laser beam (according to the pattern set by the computer) sinters certain parts of the powder bed and creates layer-by-layer PCL scaffolds.

SLS has been used to fabricate bioactive and composite PCL scaffolds with mechanical properties similar to trabecular bone. This method is suitable for making non-load-bearing PCL scaffolds (Williams et al., 2005; Doyle et al., 2015). However, due to the high temperature involved in the process, the inclusion of cells and biomaterials in SLS scaffolds is limited, and this method is only compatible with a limited number of materials (Liao et al., 2016; Liu et al., 2020b). Studies showed that SLS was not able to create a scaffold with small pores. Liu et al. (Liu et al., 2020b) fabricated PCL/hydroxyapatite scaffolds by SLS. The PCL/hydroxyapatite microspheres led to the construction of scaffolds with interconnected pores that supported cell proliferation and the penetration of blood vessels. In addition, The authors highlighted that the loading of VEGF onto the scaffolds enhanced angiogenesis and osteogenesis (Liu et al., 2020b).

SLA is one of the most expensive AM techniques, with high manufacturing accuracy and the ability to produce complex shapes with a relatively high resolution up to 1.2 μm , which uses light-activated biopolymers (Melchels et al., 2010; Ronca et al., 2021). SLA is one of the preferred printing methods, utilizing composites of photo-curable polymer (such as GelMA) in combination with PCL (Elomaa et al., 2020). The basis of SLA is light-sensitive ink photopolymerization, and the desired model is photocross-linked in each layer to form the desired 3D structure. However, due to the limited layer thickness, over-drying, and partial polymerization of the resin in the substrates, it is difficult to build micron-sized scaffolds by SLA. In addition, the presence of a photoinitiator and ultraviolet radiation sometimes causes cytotoxicity.

The cross-linking of patterns in this method does not apply shear stress to cells. The UV light source has high energy and speed for ink cross-linking, but due to its destructive effect on cell survival, the visible light source can also be used (Melchels et al., 2010; Elomaa et al., 2011a). Using solvent-free stereolithography, Elomaa

et al. (Elomaa et al., 2011b) prepared a photo-curable PCL-based resin. The resulting scaffold had high accuracy, no shrinkage, and interconnected pores of suitable size and shape.

Due to the non-uniform distribution of cells on printed scaffolds, the bioprinting method allows the simultaneous deposition and uniform distribution of living cells, macromolecules, and other biomaterials within the structures (Cunniffe et al., 2017; Genova et al., 2020). It is preferred to use PCL in combination with hydrogels containing live cells for bioprinting PCL-based scaffolds. Bioprinters typically have several printing nozzles, one for printing polymers like PCL and another for printing cells and heat-sensitive materials. This method allows the integration of various cells [such as mesenchymal stem cells (MSCs) and human umbilical vein endothelial cells (HUVECs)] into scaffolds and induces vascular formation (Genova et al., 2020; Yang et al., 2021).

The binder-jet-based printing (He, 2016), and extrusion-based printing (Borkar et al., 2021) are also used in preparing the PCL composite scaffolds. It should be noted that the use of PCL alone is not recommended in bioprinting and encapsulation, as this polymer is a hydrophobic material with a destructive temperature and viscosity for cells and requires high pressure for printing. Hence, by using co-printing and its combination with suitable polymers, the desired properties of this polymer can also be used in bioprinting (Yu et al., 2014; Murphy et al., 2017a). Murphy et al. (Murphy et al., 2017a) fabricated a bioactive borate glass/PCL/matrigel composite containing human adipose stem cells using multi-nozzles bioprinting. Their results showed that the scaffolds had favorable bioactivity, cell survival, angiogenesis, and cellular interactions.

2.2 Optimizing 3D printing parameters

Proper ink design, selection of suitable material for bone tissue engineering, dimensions of the final model, time required for modeling, and dimensional accuracy are the most significant challenges of bioprinting (Rabionet et al., 2018a; Midha et al., 2019). Ink should be selected in such a way that it simultaneously has the necessary mechanical and physiological properties for the printing process and the bone tissue (Liu et al., 2019). Developing specific and appropriate inks and optimizing printing parameters can significantly improve the treatment of bone defects and clinical outcomes (Figure 2).

Printing parameters include two categories: design and manufacturing. Design parameters include filament diameter, deposition angle, and spacing between filaments, which determine the overall scaffold architecture. Extruder temperature, bed temperature, layer height, and deposition rate also control the printing process as fabrication parameters (Rabionet et al., 2018a; Modi and Sahu, 2021). The shape, size, interconnectivity of pores, and porosity of the scaffold affect the osteogenesis and mechanical properties of the scaffold. By adjusting the parameters of the 3D printing method, various characteristics of the scaffold can be controlled and optimized, such as pore size and shape, porosity, mechanical properties, and cell behavior (Park S. A. et al., 2018). For example, circular pores have higher fatigue resistance than triangular pores (Gong et al., 2017). Five-angle scaffolds under compressive loading have less stiffness than three-angle scaffolds.

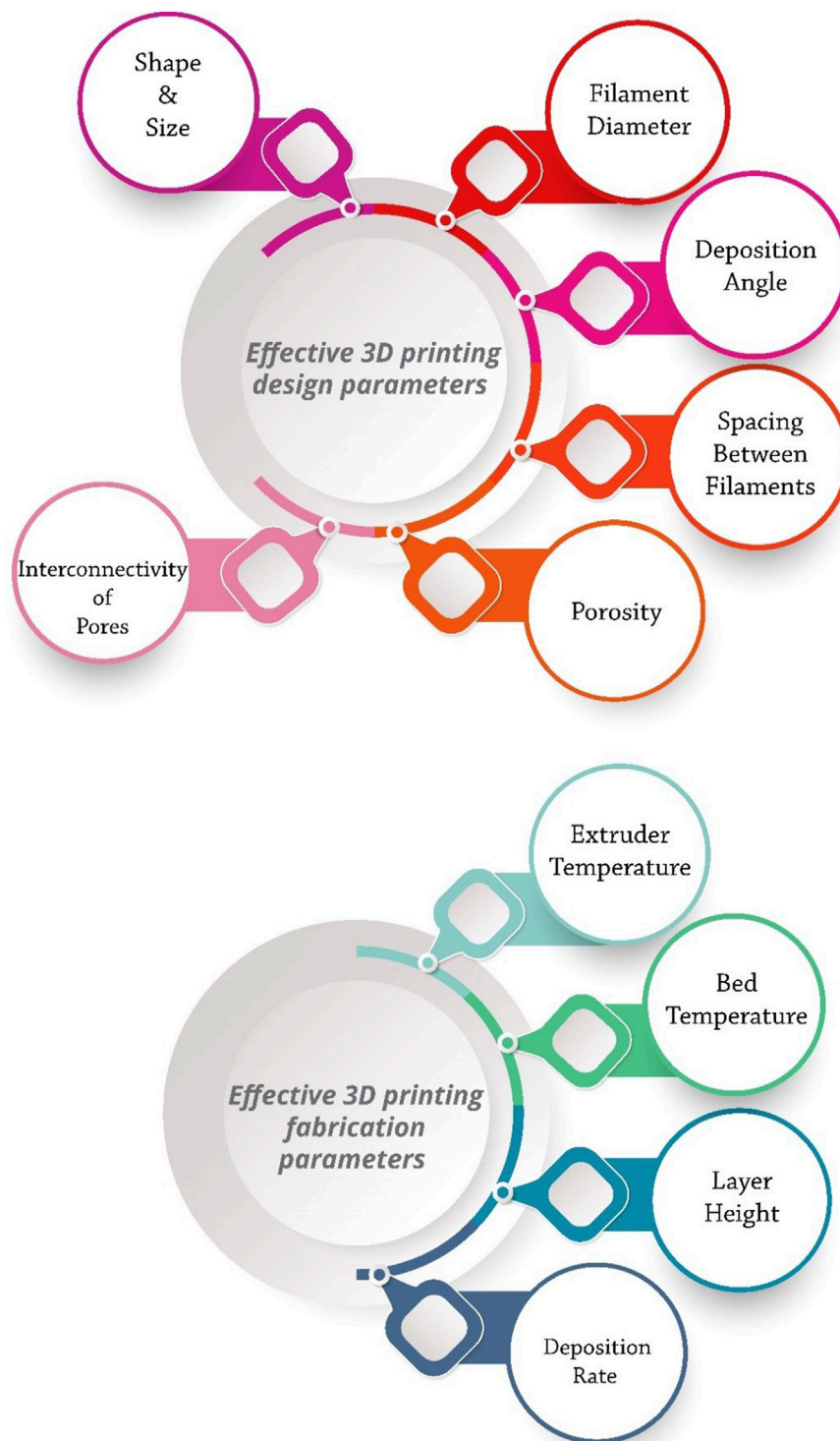


FIGURE 2
Effective 3D printing parameters for fabricating the PCL-based scaffolds.

Even the deposition angle of scaffold layers can affect cellular responses. For example, a study showed that 0° , 60° , and 120° stimulated cell proliferation better than 0° , 72° , 144° , 36° , and 108° in the first 2 weeks, but after three and 4 weeks, the results were quite the opposite (Rabionet et al., 2018b).

In BTE, there must be an optimal balance between pore size and the mechanical strength of the scaffold. The number and height of the printed layers are also quite influential. The layer's height is inversely related to the printing speed and dimensional accuracy (Pazhouhnia et al., 2022). The thickness of each layer must be greater

than the porogen particles to ensure proper bonding of the layers. On the other hand, excessive layer height leads to extensive z steps. The layer's height is controlled by the nozzle's diameter (Zhao D. et al., 2020; Modi and Sahu, 2021).

In addition, various PCL-based ink preparation methods for printing also affect the printability, swelling/degradation, and mechanical properties of scaffolds. Melt-blending, powder blending, liquid solvent technique, and solid solvent technique are standard strategies for preparing PCL-based inks (Zimmerling et al., 2021). The solvent or combination of solvents is a crucial factor in their scaffold properties. Various solvents have multiple interactions with PCL and have diverse volatility, protein conductivity, and dispersion of particles, resulting in individual uniformity and structural order.

3 PCL-based composites

PCL-based scaffolds were introduced more than decades ago for BTE (Beheshtizadeh et al., 2020). These scaffolds were implanted in more than 20,000 patients and helped repair bone defects (Teoh et al., 2019). As mentioned previously, PCL is a Food and Drug Administration (FDA)-approved linear thermoplastic and aliphatic polyester with high biocompatibility, low cost, easy processing, non-carcinogenicity, low immunogenicity, a slow degradation rate, and lower acid degradation products compared to other polyesters (Malikmammadov et al., 2018; Malikmammadov et al., 2019; Bikuna-Izagirre et al., 2022). This semi-crystalline polymer has sufficient potential for use in high-load-bearing bones (Lee et al., 2011).

Despite the beneficial properties mentioned for PCL, its hydrophobicity, low bioactivity, and slow degradation rate

remain major challenges in biomedical applications. Mixing or copolymerizing PCL with other components leads to altered mechanical, surface, and physicochemical properties of the scaffold. In this regard, various research has used the combination of diverse metals, ceramics, and polymers with PCL to improve its features, which will be discussed in detail in this section (Table 2).

3.1 PCL/ceramic composites

Ceramics are generally hard, wear-resistant, oxidation-resistant, thermal-resistant, inert, and brittle materials with low tensile strength and high compression strength (Jonathan Black, 1998; Farid, 2019). PCL/ceramic composite materials possess a higher level of mechanical properties, bioactivity, hydrophilicity, and biodegradability compared to pure PCL (Fathi-Achachelouei et al., 2019; Biscaia et al., 2022b). Hydroxyapatite (Biscaia et al., 2022b), carbon nanotubes (CNTs) (Gonçalves et al., 2016), β -tricalcium phosphate (β -TCP) (Park H. et al., 2018), graphene (Wang et al., 2016b; Zhang et al., 2018a) and mesoporous bioactive glasses (Zhang et al., 2018a) are the most commonly used ceramic materials in combination with PCL.

Hydroxyapatite ($\text{Ca}_{10}(\text{PO}_4)_6(\text{OH})_2$, HAp) is a ceramic material whose composition and structure are similar to the mineral part of natural bone. This substance plays a pivotal role in strengthening the proliferation of bone cells, increasing protein absorption, improving cell adhesion, and preventing the growth of cancer cells (Hassanajili et al., 2019b; Biscaia et al., 2022b; Rezanian et al., 2022b). The addition of HAp to PCL improves biocompatibility, osteoconductivity, bone integration, and the mechanical properties of the composite. HAp has a dense crystalline structure and induces bone matrix mineralization *in vivo*

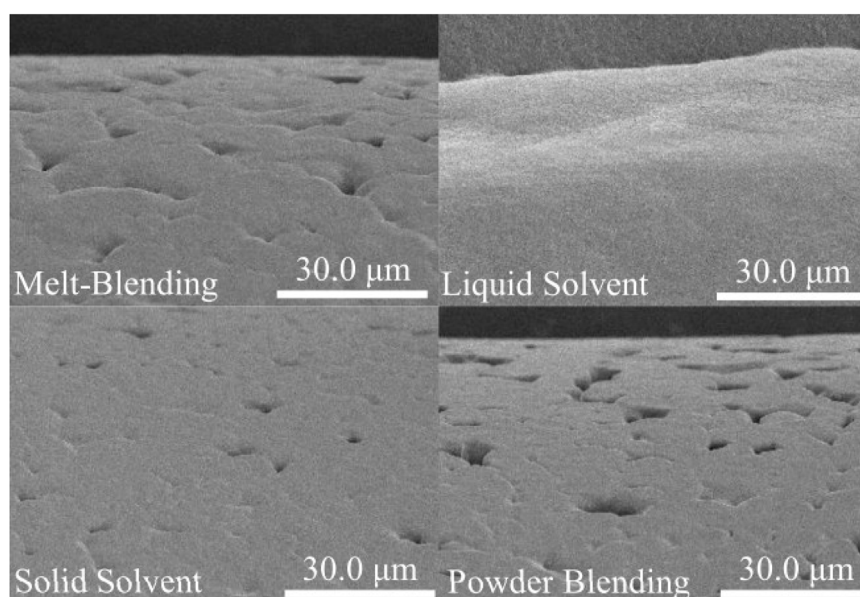


FIGURE 3

The effect of the preparation method on the SEM images of 3D-printed PCL-HAp filaments (1500X magnification), reprinted with permission from (Zimmerling et al., 2021). Scaffolds prepared with powder blending had the deepest and largest number of pores on the surface of the filaments, and scaffolds based on liquid solvent had a smooth surface due to the lower viscosity of the liquid and the filling of the pores by materials during printing.

TABLE 2 Some recent studies on PCL-based composites in BTE applications.

	Material	Printing parameters	Animal model	Cell/biomolecule	Outcomes	Ref
PCL/ceramic composites	PCL	• Extrusion-based technique	Rat, tibial defect (8 mm)	Alendronate	• Sustained release of alendronate	Kim et al. (2016a)
		• Liquid solvent technique			• Improved ALP activity and calcium deposition	
		• Speed and air pressure: 5 mm s ⁻¹ and 80 kPa			• Increased new bone formation and mineralization	
		• Nozzle size: 25-G				
	PCL/Strontium- and cobalt- doped bioactive glass	• 30% porosity	-	-	• PCL/Strontium- and cobalt- doped bioactive glass improve Young's modulus, apatite-forming ability, and cytocompatibility	Fathi et al. (2020)
		• Nozzle size and temperature: 500 μm and 120 °C				
		• spacing between the filaments: 400 μm				
	PCL/nanoparticulate Willemite	• Liquid solvent technique	Rabbit, Femoral defect (Osteonecrosis model)	-	• PCL/npW improved cytocompatibility, osteogenic activity, and HA accumulation	Karimzadeh Bardeei et al. (2021)
		• Temperature 75°C, pressure 3.38 bar				
		• Speed 6 mm/min				
PvCL/Bioactive borate glasses	• Extrusion-based Liquid solvent technique	-	-	• Adipose stem cells	• Improve angiogenesis and bioactivity	Murphy et al. (2017a)
	• Scaffolds 10 × 10 × 1 mm ³				• Sustained release of bioactive glass	
	• pore sizes 100–300 μm				• 60% cell viability	
	• pressure 10–50 psi, nozzle size 110–600μm					
PCL/HA	• Extrusion-based technique	-	-	-	• The mechanical characteristics and crystallinity of the scaffold were improved by HA.	Biscaia et al. (2022a)
	• Melt blending and solvent casting preparation				• In comparison to solvent casting ink preparation, melt blending ink preparation has improved mechanical qualities, cytocompatibility, and osteogenic potential	
	• Deposition velocity: 300 mm/min					
	• Screw rotation velocity 10–20 rpm					
	• Melting temperature 70–80°C					
PCL/HA	• SLS technique	Rat, Calvarial Defect (5mm diameter)	VEGF	• Enhanced blood vessel formation	Liu et al. (2020b)	
				• Enhanced <i>in vivo</i> bone regeneration		
PCL/HA	• FFF techniquepore size 400 μm	-	-	-	• Young's modulus has been increased by 50%	Rezania et al. (2022a)
	• nozzle size 0.4 mm				• Biocompatibility, Alkaline phosphatase (ALP) activity, and calcium deposition all improved after HA was added	
	• nozzle and ambient temperatures: 180 °C and 25°C					
PCL/nHa	• Extrusion-based technique	-	-	-	• The best printability, lowest swelling/degradation, and consistent mechanical qualities come via melt blending ink preparation	Zimmerling et al. (2021)
	• Melt-blending, Powder blending, Liquid solvent technique, and Solid solvent technique				• Powder blending offers the best mechanical qualities; however, they are variable	
	• Strand diameter: 0.510 mm and a strand spacing: 1.0 mm					
	• Layer height: 80% of strand diameter					

(Continued on following page)

TABLE 2 (Continued) Some recent studies on PCL-based composites in BTE applications.

Material	Printing parameters	Animal model	Cell/biomolecule	Outcomes	Ref
PCL-HA	<ul style="list-style-type: none"> FDM technique Diameter 300 μm 	Rabbit, femoral condyle defect (6 mm diameter* depth of 6.5 mm)	Heparan sulfate	Optimal concentration of heparan sulfate increased Biocompatibility, promoted osteoblast maturation and new bone formation, and high compression resistance	Liu et al. (2020a)
	<ul style="list-style-type: none"> Pore size 400 μm, 20 layers 			high concentration of heparan sulfate inhibited (500 $\mu\text{g/mL}$) osteoblast maturation	
PCL/HA/CNT	<ul style="list-style-type: none"> Extrusion-based technique 	-	-	<ul style="list-style-type: none"> Addition of 0.75% CNT increased the compressive yield stress (6.5 MPa) 	Goncalves et al. (2016)
	<ul style="list-style-type: none"> Liquid solvent technique 				
	<ul style="list-style-type: none"> Pore size: 450–700 μm 			<ul style="list-style-type: none"> 2 wt% CNT scaffold has the best mechanical and electrical properties 	
	<ul style="list-style-type: none"> Needle diameter: 0.45 mm 			<ul style="list-style-type: none"> HA/CNT improve protein adsorption, cell adhesion, and bioactivity 	
PCL/ β -TCP	<ul style="list-style-type: none"> Extrusion-based technique 	-	-	<ul style="list-style-type: none"> Improved osteogenic differentiation and expression of related genes and proteins 	Park et al. (2018a)
	<ul style="list-style-type: none"> Melt-blending 				
	<ul style="list-style-type: none"> Nozzle diameter: 300 μm 				
PCL/ β -TCP	<ul style="list-style-type: none"> Extrusion-based technique Nozzle diameter: 400 μm 	Dogs, mandibular defect (10.0 \times 5.0 \times 5.0 mm)	rhBMP-2	<ul style="list-style-type: none"> Increased ALP activity, mineralization, new bone formation, and biodegradability 	Park et al. (2021a)
	<ul style="list-style-type: none"> Scaffolds dimensions: 10 \times 4 \times 4 mm³ 				
PCL/ β TCP	<ul style="list-style-type: none"> Extrusion-based technique 	Pigs, Mandibular defects (2 cm/2 cm)	Porcine bone marrow progenitor cells (pBMPC)	<ul style="list-style-type: none"> Increased new bone formation 	Konopnicki et al. (2015)
	<ul style="list-style-type: none"> Micropore (5–40 μm) and macropore (70–300 μm) 				
PCL/ β -TCP	<ul style="list-style-type: none"> FDM technique 	-	-	<ul style="list-style-type: none"> Increasing the β-TCP can increase the surface roughness, osteogenic differentiation, and degradation rate 	Bruyas et al. (2018a)
	<ul style="list-style-type: none"> Solvent Casting preparation 			<ul style="list-style-type: none"> Increasing the β-TCP can decrease the contact angle 	
	<ul style="list-style-type: none"> Printing speed: 5 mm/s 			<ul style="list-style-type: none"> Increasing the β-TCP and decreasing the scaffold porosity can increase the Young's modulus 	
	<ul style="list-style-type: none"> Printing temperature: 160°C 				
	<ul style="list-style-type: none"> Struts width: 350 μm–400 μm 				
PCL/ β -TCP	<ul style="list-style-type: none"> FDM and Melt-electrowriting 	-	-	activity, and calcium deposition are all improved. A fine fiber grid inserted in the pores of thick fibers can guide cells across bridges and cover the pores.	Wang et al. (2021)
	<ul style="list-style-type: none"> Solvent Casting preparation 				
	<ul style="list-style-type: none"> Cross-scale scaffold (coarse fiber mesh (500 μm), and fine fiber meshes (10 μm)) 				
PCL/pristine graphene	<ul style="list-style-type: none"> Extrusion-based technique 	-	-	<ul style="list-style-type: none"> Improved cell viability, proliferation, and hydrophilicity 	Wang et al. (2016a)
	<ul style="list-style-type: none"> Melting temperature 90°C, slice thickness 220 μm, deposition velocity 20 mm/s 				
PCL/graphene oxide	<ul style="list-style-type: none"> Extrusion-based 	-	-	<ul style="list-style-type: none"> Cell attachment, proliferation, ALP activity, and mineralization were increased by adding a small amount of GO 	Unagolla and Jayasuriya (2019)
	<ul style="list-style-type: none"> Solvent Casting preparation 				

(Continued on following page)

TABLE 2 (Continued) Some recent studies on PCL-based composites in BTE applications.

	Material	Printing parameters	Animal model	Cell/biomolecule	Outcomes	Ref
		<ul style="list-style-type: none"> • 5 × 5 mm mesh, pore sizes (400 μm, and 800 μm), 22 layer, nozzle size: 0.159 mm, temperature 100 °C • Speed 1 mm/s, printing pressure 80–100 PSI 			<ul style="list-style-type: none"> • Smaller pore size showed a higher compressive modulus 	
	PCL/Ca-polyphosphate-microparticles	<ul style="list-style-type: none"> • Extrusion-based technique • Powder blending • Temperature 100 °C, scaffolds 10 mm diameter * 1.5 mm height, layer thickness 320 μm • Pressure 7.8 bar, speed 3 mm/s 	-	-	<ul style="list-style-type: none"> • Improve cell attachment, bone remodeling, and hydroxyapatite deposition 	Neufurth et al. (2017)
PCL/polymer/ceramic composites	PCL/β-TCP/Porcine-bdECM	<ul style="list-style-type: none"> • Extrusion-based technique 	Rats, calvaria defect (8 mm diameter)	rhBMP-2	PCL/β-TCP/bdECM/BMP scaffold improved bioactivity, new bone formation, and cell adhesion	Bae et al. (2018b)
		<ul style="list-style-type: none"> • Melt-blending and Liquid solvent technique 				
		<ul style="list-style-type: none"> • Line width: 300 μm, pore size: 400 μm, and line height: 100 μm 				
		<ul style="list-style-type: none"> • Scaffold dimensions: 7 × 7 × 1 mm³ 				
	PCL/bdECM/β-TCP	<ul style="list-style-type: none"> • Extrusion-based technique • Nozzle size: 500 μm 	Rat, calvarial defects (8-mm diameter)	-	<ul style="list-style-type: none"> • Combination of PCL/bdECM/β-TCP improve osteogenic potential and reduced inflammatory responses 	Yun et al. (2021b)
		<ul style="list-style-type: none"> • Temperature 110°C, and a pneumatic Pressure 550 kPa 				
<ul style="list-style-type: none"> • Line width 300 μm • Pore size 300μm, layer height 100 μm (4 layers) 						
PCL/β-TCP/Porcine-Derived-bdECM	<ul style="list-style-type: none"> • Extrusion-based technique 	Rabbits, skull defect, (8 mm diameter)	-	<ul style="list-style-type: none"> • Improved osteogenic potential, cell proliferation, new bone formation 	Kim et al. (2018)	
	<ul style="list-style-type: none"> • Melt blending and coating 					
	<ul style="list-style-type: none"> • Temperature 120 °C, pneumatic pressure 500 kPa, scaffold dimension 8 mm diameter * 2 mm height, line width 300 μm 					
	<ul style="list-style-type: none"> • Pore size 300 μm, and line height 100 μm 					
Magnesium calcium silicate/gliadin/PCL	<ul style="list-style-type: none"> • Extrusion-based technique 	Rabbits, femoral defects (5 mm)	-	<ul style="list-style-type: none"> • Addition of magnesium calcium silicate and gliadin improved the compressive strength, cell attachment, cell proliferation, new bone volume, and degradability 	Zhang et al. (2018b)	
	<ul style="list-style-type: none"> • Liquid solvent technique 					
	<ul style="list-style-type: none"> • Temperature 130°C, speed 100 mm/min, nozzle size 0.33 mm, line width 500 μm 					
	<ul style="list-style-type: none"> • Pore size 500 μm, line height 500 μm 					
PCL/PLGA/-TCP	<ul style="list-style-type: none"> • Extrusion-based technique 	Rabbits, calvarial defects (8 mm)	rhBMP-2	<ul style="list-style-type: none"> • Improve new bone formation • Sustained drug release 	Shim et al. (2014)	
	<ul style="list-style-type: none"> • Melt-blending and Liquid solvent technique 					
	<ul style="list-style-type: none"> • Circular scaffold (10 mm diameter) 					

(Continued on following page)

TABLE 2 (Continued) Some recent studies on PCL-based composites in BTE applications.

	Material	Printing parameters	Animal model	Cell/biomolecule	Outcomes	Ref
		<ul style="list-style-type: none"> ● Head1:temperature 135C and pressure 650 kPa, head 2: temperature 20C and pressure 30 kPa 				
	PCL/PLGA/-TCP	<ul style="list-style-type: none"> ● Extrusion-based technique Temperature 135C and pressure 650 kPa ● Strut width 300 μm, pore size 200 μm, porosity 40% 	Beagle, edentulous mandibular alveolar ridge		<ul style="list-style-type: none"> ● Conserved mechanical properties in wet and dry conditions ● Appropriate biocompatibility and bone regeneration (similar to collagen membrane) 	Won et al. (2016)
	PCL/hydrogel (alginate/gelatin/nano-hydroxyapatite)	<ul style="list-style-type: none"> ● FDM technique ● Melt-blending ● Nozzle size: 0.4 mm, temperature 110C, speed 90 mm/s 	-	hMSC	<ul style="list-style-type: none"> ● Improved bioactivity, cytocompatibility, mineralization, and osteoconductivity ● In comparison to 3D printed mesh and honeycomb scaffolds, the printed gyroid scaffold of PCL enabled for a greater amount of hydrogel to be loaded within the scaffolds 	Hernandez et al. (2017a)
	PCL/Gelatin/Bacterial Cellulose/Hydroxyapatite	<ul style="list-style-type: none"> ● FDM technique ● Liquid solvent technique ● Pore size 300 μm, nozzle size 0.5mm, flow rate 0.2 mL/h, 10 Layers, Platform Temperature 38C 	-	-	<ul style="list-style-type: none"> ● Improve cell attachment and proliferation ● Both the optimal pore size for bone tissue engineering and a uniformity ratio of more than 90% are found in the 80 percent infill rate 	Cakmak et al. (2020)
	PCL/TCP/methacrylated hyaluronic acid/methacrylated gelatin	<ul style="list-style-type: none"> ● Extrusion-based technique ● Liquid solvent technique ● Scaffold 20 mm × 20 mm × 1 mm 	Rat, mandibular defect (4 mm)	Resveratrol and Strontium ranelate	<ul style="list-style-type: none"> ● Resveratrol had a more sustained release profile, while Strontium ranelate had an initial burst release then a sustained release ● SrRn increase cell proliferation and osteogenic potential ● Scaffolds decrease osteoclast activity 	Zhang et al. (2020)
PCL/polymer composites	PCL/polyaniline	<ul style="list-style-type: none"> ● Extrusion-based technique ● Melt compounding ● Nozzle size 330μm, speed 20 mm s⁻¹, temperature 90°C, pressure 6 bar 	-	-	<ul style="list-style-type: none"> ● Polyaniline increase the scaffold conductivity ● Scaffold with 0.1% wt. polyaniline has the suitable conductivity and mechanical properties for bone healing ● 1% and 2% wt. polyaniline has cytotoxic effect 	Wibowo et al. (2020)
	Pcl/GelMA	<ul style="list-style-type: none"> ● Extrusion-based technique ● Melt-blending and Liquid solvent technique ● The printing platform temperature 10C ● Head 1: speed 10 mm/s and pressure 1.8 bar ● Head 2: speed 2 mm/s and pressure: 7.3 bar nozzles size: 400 μm 	-	Dental pulp stem cells	<ul style="list-style-type: none"> ● Improve compressive modules to human trabecular bone ● 90% cell viability ● Improved osteogenic differentiation and mineralization 	Buyuksungur et al. (2021a)
	levan/polycaprolactone/gelatin	<ul style="list-style-type: none"> ● FDM technique ● Liquid solvent technique 	-	-	<ul style="list-style-type: none"> ● Levan increase biocompatibility ● Levan decrease surface tension and compressive strength of the scaffolds 	Duymaz et al. (2019)

(Continued on following page)

TABLE 2 (Continued) Some recent studies on PCL-based composites in BTE applications.

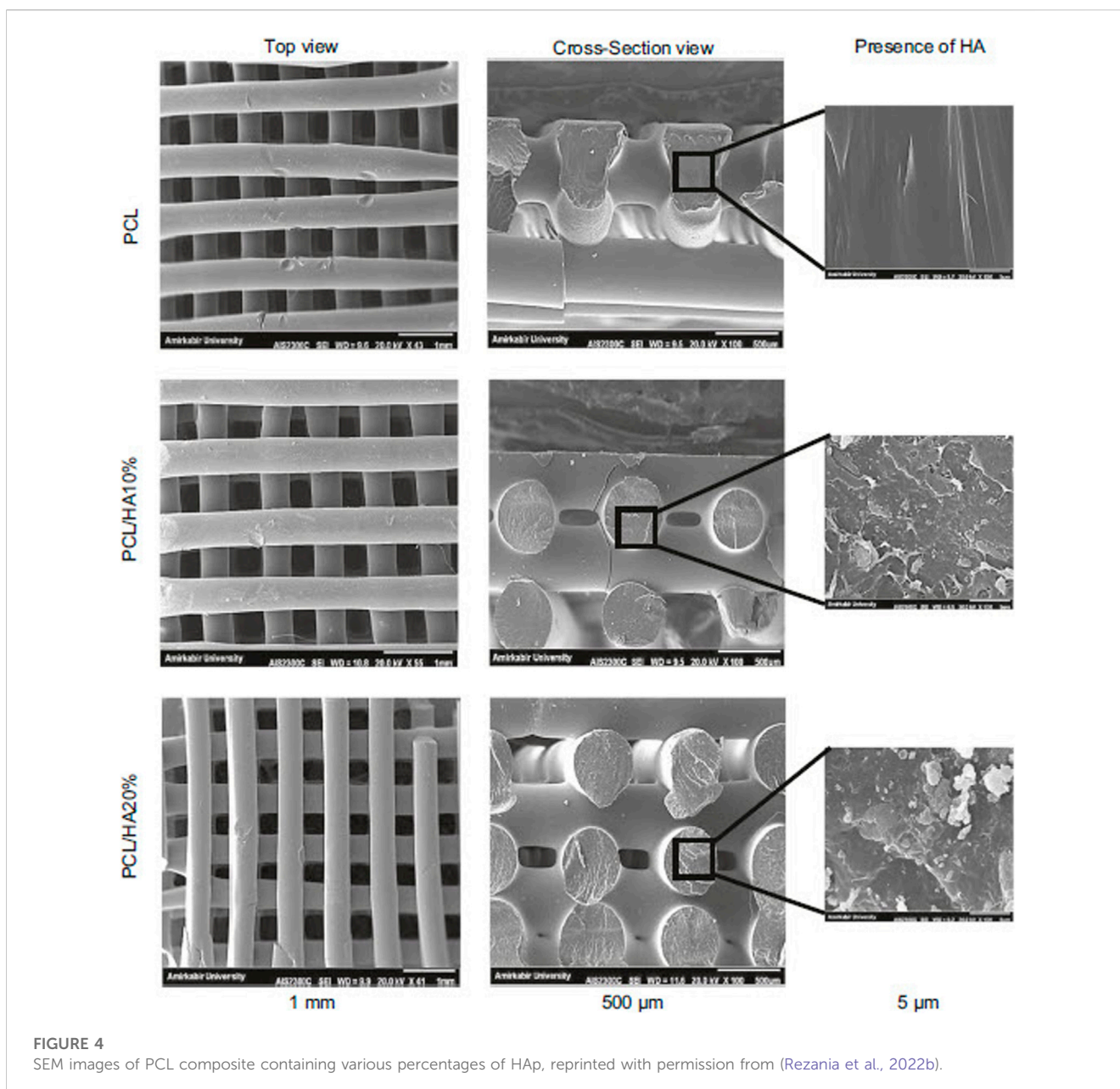
	Material	Printing parameters	Animal model	Cell/biomolecule	Outcomes	Ref
		Nozzle size 0.4 mm, the build plate temperature 45°C–55 °C, travel speed 100–150 mm.s ⁻¹				
	PCL/gelatin	● Extrusion-based technique	-	-	● Gelatin improve hydrophilicity, pore size distribution, interconnectivity, and osteogenic differentiation	Azarudeen et al. (2020)
		● Liquid solvent technique				
		● Strut size 0.4 mm, temperature 24 °C, pressure 2.5 bar, speed 30 mm/s				
	PCL/fish bone extract	● Extrusion-based technique	-	-	● Improved cell proliferation, osteogenic differentiation, and calcium deposition	Heo et al. (2019a)
		● Melt blending and coating				
		● Temperature 110C, nozzle size 400 μm				
		● Pressure 500 kPa, velocity 0.2 mm/s				
PCL/metal composites	PCL/Mg	● FDM technique	Rabbits, medial tibial tubercle defect (6 mm diameter *4.5 mm depth)	-	● Biom mineralization, biocompatibility, new bone formation, and biodegradability were all increased by magnesium	Dong et al. (2021)
		● Temperature 160°C, speed 1.5 mm.s ⁻¹				
	PCL/Mg	● FDM technique	Rat, skull defect (8 mm)	-	● PCL/10% Mg improve hydrophilicity, cell proliferation, osteogenic activity, new bone formation	Zhao et al. (2020a)
		● Scaffold dimension 8 mm diameter* 1.5 mm height, wire diameter 200 μm				
● Temperature 110 °C, pressure 0.6 MPa, speed 6–8 mm/s						
PCL/Zn	● FDM technique	Rats, calvaria defect (6 mm)	-	● Zn improved mechanical properties and cytocompatibility	Wang et al. (2022d)	
	● Melt- compounding (filaments fabrication)					
	● Nozzle size 300 μm , speed 500 mm/min, layer thickness 300 μm, pore size 300 μm, porosity 50%					
					● 2 wt% Zn improved osteogenic potential	
					● increase of Zn can increase osteoclastogenesis	

while preventing the formation of fibrotic tissue (Huang et al., 2018; Hassanajili et al., 2019b; El-Habashy et al., 2021). The HAp nanoparticles increase differentiation, bone cell proliferation, mineral deposition, and ultimately accelerate the formation of bone tissues (Figure 4) (Gatto et al., 2021; Zimmerling et al., 2021).

Studies showed that the addition of β -TCP (as an osteoconductive material) to PCL improved its biodegradability (more effective than HAp), mechanical strength, and binding ability of the resulting composite to proteins, growth factors, and cells (Kim Y. et al., 2016; Park H. et al., 2018). The double holes on the TCP surfaces allow the penetration of vascular and bone tissue inside the resulting composite (Tarafder and Bose, 2014; Park H. et al., 2018). Broyas et al. (Bruyas et al., 2018b) investigated the effect of the ceramic material on the properties of the resulting composite by adding 0–60 wt% of β -TCP to PCL. They found that the addition

of β -TCP could improve the mechanical properties, biodegradability, and surface properties of the bone scaffold. Huang et al. (Huang et al., 2018) investigated the effect of adding both HAp and β -TCP ceramic materials to PCL. According to their results, the addition of HAp improved the biological and mechanical properties of the resulting composite more than the addition of TCP.

CNTs are materials with known chemical, electrical, mechanical, and structural properties, while their combination with PCL improves the electrical conductivity of the resulting composite and induces bone healing (Peidavosi et al., 2022). Carbon nanotubes are often used as imaging agents and carriers of bioactive molecules (Saito et al., 2008; Gonçalves et al., 2016; Weselucha-Birczyńska et al., 2021). Also, graphene is another ceramic material whose combination with PCL improves its processability, cell attachment, mechanical properties, biological function, and conductivity. However, in terms of



cytotoxicity, the use of graphene is challenging, and some studies have shown toxic effects at high doses (Figure 5) (Niyogi et al., 2006; Wang et al., 2016b).

3.2 PCL/polymer composites

Polymers are divided into two categories, including synthetic and natural. Semi-crystalline or amorphous synthetic polymers are biodegradable, biocompatible, non-immunogenic, and non-toxic. Synthetic polymers are produced under controlled conditions and thus have tunable mechanical properties, crosslinkability, Young's modulus, and degradability (Middleton and Tipton, 2000; Hassanajili et al., 2019b). In contrast, natural polymers have higher degradation rates, lower mechanical properties, and better cell binding; however, they have batch-to-batch variations (Bharadwaz and Jayasuriya, 2020). The combination of various natural and synthetic polymers, along with decellularized tissues, with PCL could improve its features.

Poly(lactic acid) (PLA) is one of the most widely used synthetic polymers, which is converted into non-toxic components utilizing a controlled degradation rate. PLA has a more brittle structure, a faster degradation rate, and less flexibility compared to PCL (Hassanajili et al., 2019b). Combining PLA with PCL could overcome the limitations of both polymers, such as brittleness, degradation rate, and cellular attachment efficiency. Xu et al. (Xu et al., 2018) used various composition ratios of PLA/PCL to improve the osteogenic differentiation of hMSCs. By increasing the weight ratio of PLA (up to 80%), the

stiffness, bioactivity, and osteogenic potential of the 3D PCL/PLA scaffold were improved. Increasing the weight ratio of PLA led to an improvement in alkaline phosphatase activity and calcium content.

(Poly (lactic-co-glycolic) acid) (PLGA) is a biocompatible and biodegradable synthetic polymer, suffering from poor mechanical properties. The notable fact is that its by-products create an acidic environment (Shim et al., 2015). A study showed that the PCL/PLGA/ β -TCP printed scaffold improved bone healing (Hwang K. S. et al., 2017). This composite possessed favorable biological and mechanical properties of PCL and PLGA, along with the osteoconduction feature of β -TCP. The authors emphasized that the 3D printing technique could produce this composite with various thicknesses and pore sizes (Hwang K. S. et al., 2017).

Polyphosphate is an inorganic and physiological polymer found in platelets, serum, and metazoans. This polymer has favorable morphogenetic and biocompatible activity and stimulates anabolic signals and metabolic processes, increasing adenosine triphosphate (ATP) synthesis and hydroxyapatite formation. However, it has poor mechanical properties, and its combination with PCL leads to the creation of a composite with favorable mechanical properties, biocompatibility, and morphogenetic activity for bone tissue repair (Müller et al., 2015; Neufurth et al., 2017).

Gelatin is a natural polymer derived from collagen, which has been used in combination with multiple synthetic polymers, including PCL, due to its low cost, availability, biocompatibility, suitable functional groups, enzymatic biodegradability, and low immunogenicity. Studies have approved that combining gelatin

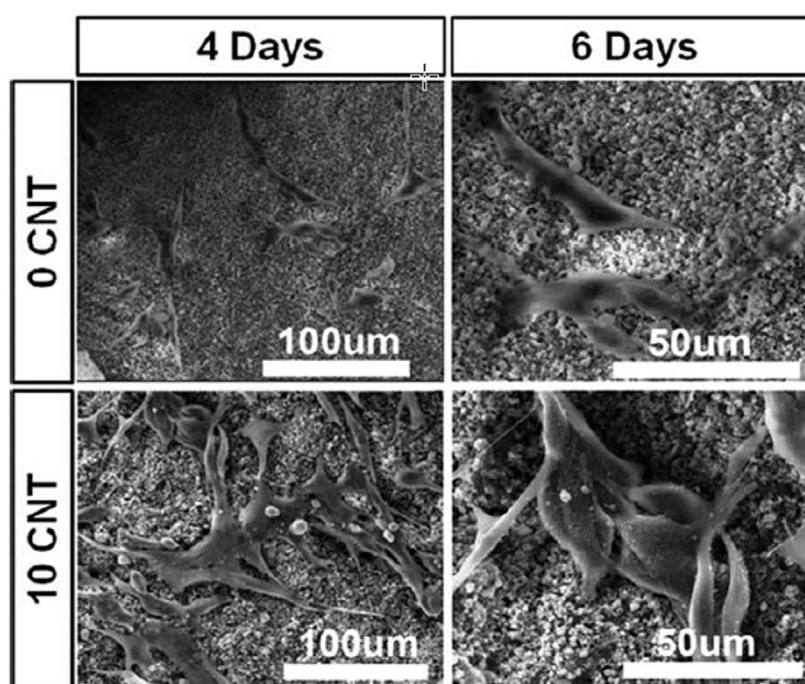


FIGURE 5

The effect of CNT amount on the attachment of MG63 cells in PCL-CNT composite scaffold, reprinted with permission from (Gonçalves et al., 2016).

with PCL stimulates osteogenic differentiation and improves the degradation rate of PCL (Buyuksungur et al., 2021b; El-Habashy et al., 2021).

Bone ECM contains a variety of collagens, proteoglycans, growth factors, and non-collagenous proteins; hence, acellular tissues can help in improving intercellular connections, proliferation, and cell differentiation (Bolander and Balian, 1986; Pati et al., 2014). Combining the decellularized bone matrix (bovine or cadaver) with PCL creates a ink that can help promote bone regeneration, cell adhesion, and osteoblast proliferation via accelerating the osteoconductive and osteoinductive signaling procedures (Bae E. B. et al., 2018; Yun et al., 2021a).

Not only, the research investigated that fish bone extract has anticoagulant, antibacterial, and antioxidant properties, but also possesses the ability to increase alkaline phosphatase activity (Heo et al., 2019a). The combination of the fish extract with PCL improves osteogenic effects and improves the mineralization of bone tissue (Heo et al., 2018; Heo et al., 2019b). Heo et al. (Heo et al., 2019a) used a coating of fish bone extract on a 3D-printed PCL scaffold to improve its osteogenic properties. Their results showed that the resulting scaffold improved the adhesion and proliferation of MC3T3-E1 cells and promoted the expression of osteogenic genes and

calcium deposition (Figure 6). Also, gliadin is a natural polymer of wheat protein with favorable mechanical properties and degradability, and its combination with PCL and bioglass can stimulate the proliferation and differentiation of bovine turbinate fibroblasts and the growth of bone tissue (Reddy and Yang, 2008; Zhang et al., 2018a).

3.3 PCL/metal composites

Metals have appropriate strength and toughness, while some challenges, such as stress shielding (mismatching the elastic modulus of metals and natural bone), higher stiffness (decreasing bone density), a slow degradation rate, and the need for a second surgery (to remove excess metal material) have limited their usage. Therefore, the combination of metals with biodegradable polymers such as PCL increases the potential of their application in bone repair (Ciosek et al., 2021; Raj Preeth et al., 2021; Huber et al., 2022). Magnesium (Zhao et al., 2020c), Zinc (Wang S. et al., 2022), and Silver (Shao et al., 2019a) are the most commonly used metals in combination with PCL for bone repair.

Magnesium (Mg) is a biodegradable metal with high mechanical properties and FDA approval (Han et al., 2019). Magnesium is

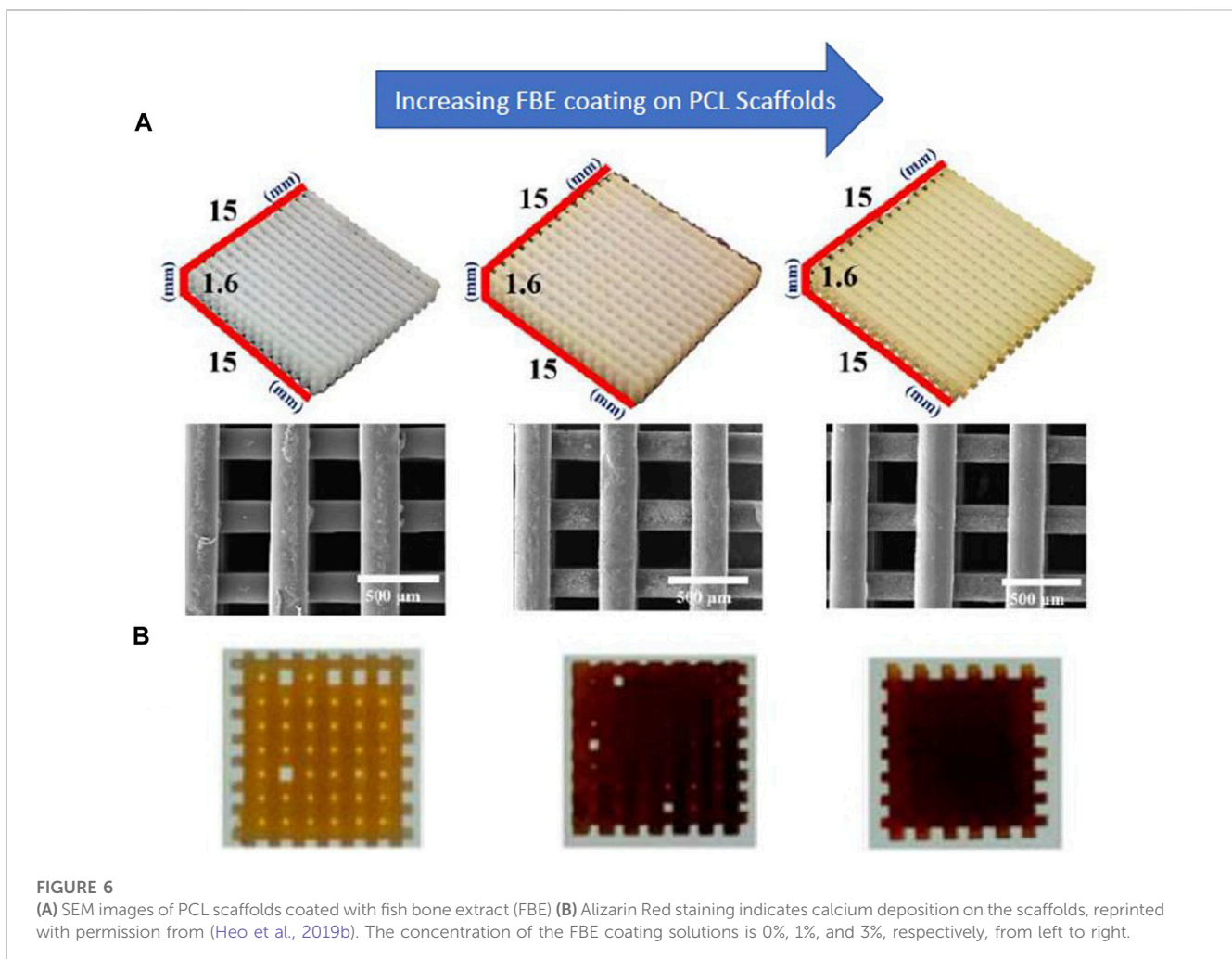


FIGURE 6

(A) SEM images of PCL scaffolds coated with fish bone extract (FBE) (B) Alizarin Red staining indicates calcium deposition on the scaffolds, reprinted with permission from (Heo et al., 2019b). The concentration of the FBE coating solutions is 0%, 1%, and 3%, respectively, from left to right.

involved in angiogenesis, antibacterial effects, proosteogenic effects, protein synthesis, oxidative phosphorylation, and mineralization of bone tissue (Roh H. S. et al., 2017; Peng et al., 2021). Studies showed that magnesium stimulated the differentiation of osteoblasts (Wang J. et al., 2017). The composition of magnesium in PCL can increase the bioactivity, degradation rate, and mechanical properties of the resulting composite according to the needs of bone tissue (Zhao et al., 2020c).

Zinc (Zn) is a metal with favorable mechanical strength, biocompatibility, and degradation rate, and its decomposition products do not contain hydrogen gas (Maleki-Ghaleh et al., 2021; Wang S. et al., 2022). Zn is involved in energy metabolism, angiogenesis, protein synthesis, collagen synthesis, bone formation, and mineralization (Ghorbani et al., 2015; Li et al., 2019). The combination of Zn and PCL can improve mechanical properties and osteogenesis. Studies have shown that 1–50 μM of Zn is favorable for osteogenesis, and doses of more than 50 μM inhibit osteogenesis (Wang S. et al., 2022).

4 Incorporation of cells in scaffolds

To integrate living cells into PCL-based scaffolds during printing, bioinks and bioprinter devices described in Section 2.1 are used. Bioink includes a mixture of several biomaterials (generally in the form of hydrogel) and desired cell types, which are used under specific conditions of bioprinters to create tissue constructs (Borkar et al., 2021). Cell-laden bioinks enable the creation of functional tissues from various cells and biomaterials. The possibility of integrating the patient's cells into the bioink reduces the risk of transplant rejection (Beheshtizadeh et al., 2022). Cell encapsulation provides homogeneous cell seeding and suitable anchorage, which leads to proper cell signaling, cell function, and tissue repair. The combination of PCL with various cells in the bioprinting process increases the clinical application of the resulting scaffolds (Murphy et al., 2017b; Buyuksungur et al., 2021b).

Buyuksungur et al. (Buyuksungur et al., 2021b) used the combination of PCL and GelMA containing dental pulp stem cells (DPSCs) for BTE applications. The cell-containing hydrogel was printed between the PCL struts. The resulting scaffolds had osteoinduction properties (due to cell-loaded GelMA), sufficient mechanical strength (due to PCL), and a compressive modulus similar to trabecular bone's modulus. The cells in this structure had a high survival rate (over 90%) and were uniformly distributed. The authors claimed that this scaffold supported bone differentiation and mineral deposition.

Murphy et al. (Murphy et al., 2017b) printed the scaffold composed of PCL and borate glass, which contained human adipose stem cells (ASCs). The separated nozzle was used to print ASCs suspended in Matrigel. While the ASCs possess a high viability, the authors pointed that the angiogenesis rate increased with the increasing borate glass. This bioactive scaffold was introduced for BTE applications. Also, in another study, Hernandez et al. (Hernandez et al., 2017b) used a combination of hydrogel (alginate and gelatin) containing human MSCs with PCL for bioprinting. The scaffold had favorable cytocompatibility, cell adhesion and viability, bioactivity, and the growth of apatite crystals.

Pati et al. (Pati et al., 2015b) created a bone microenvironment by printing PCL/PLGA/ β -TCP/decellularized ECM containing nasal inferior turbinate tissue-derived MSCs. Based on the researchers' report, scaffolds supported the osteoblastic differentiation of cells and enjoyed increased calcium deposition. They reported that the scaffolds increased the expression of RUNX2, osteocalcin, alkaline phosphatase, and osteopontin (about four times).

Moreover, Dong et al. (Dong et al., 2017) encapsulated rabbit bone marrow MSCs and BMP-2 in chitosan hydrogel and then printed the combination of this hydrogel and PCL. The cells had an appropriate survival rate, and a uniform distribution of them was reported in the structure. Furthermore, scaffolds had osteogenic, osteoconductive, and bone matrix formation properties, as well as the mechanical strength necessary for BTE applications.

5 Incorporation of angiogenic and osteogenic growth factors in scaffolds

Various drugs and growth factors are integrated into the printed scaffold to increase bioactivity, osteogenesis, angiogenesis, osteoclast prevention, and bone regeneration. In addition, it avoids the issues associated with the local administration of growth factors, such as systemic toxicity, a short half-life at the injection site, and action at aberrant sites (Li et al., 2020b; Liu et al., 2020c). PCL scaffolds allow the incorporation of multiple drugs and growth factors simultaneously. These factors can be coated by physical adsorption (Park et al., 2021b) and diverse chemical agents, or incorporated (Kim S. E. et al., 2016; Bae E. B. et al., 2018) in printed PCL composite scaffolds. Multiple drugs, including aspirin (Li et al., 2020a), alendronate (Kim S. E. et al., 2016), lidocaine (Shao et al., 2019b), resveratrol (Zhang et al., 2020), strontium ranelate (Zhang et al., 2020), levofloxacin (Puppi et al., 2016a), doxorubicin (Zhang et al., 2014b), heparin sulfate (Liu Y. et al., 2020), cefazolin (Lee et al., 2022), rifampicin (Lee et al., 2022), and roxithromycin (Bai et al., 2020), along with some growth factors, such as vascular endothelial growth factor (VEGF) (Liu et al., 2020b), and bone morphogenetic proteins (BMPs) (Bae E.-B. et al., 2018), are effective in 3D-printed PCL-based composites.

VEGF is involved in angiogenesis, endothelial cell stimulation, and osteogenesis. Liu et al. (Liu et al., 2020c) modified the surface of PCL/HAP-printed scaffolds by VEGF and apatite coprecipitation. Their results showed that the VEGF improved the formation of blood vessels, osteogenic differentiation, and bone regeneration.

BMPs are transforming growth factor β (TGF- β) family members that play an important role in bone regeneration (via the Smad/MAPK pathway) and osteoblastic differentiation (Beederman et al., 2013). In addition, in the immature region of the BMP-7 protein, there is a peptide called bone-forming peptide 1 (BFP-1), which has higher osteogenesis and bone differentiation activity compared to BMP-7 (Li et al., 2020b; Park et al., 2021b). Bae et al. (Bae E. B. et al., 2018) printed PCL/ β -TCP composite containing decellularized bone and BMP-2. They reported that the presence of BMP-2 increased bioactivity and bone mass volume. Other studies showed that PCL/ β -TCP composite is a better carrier for BMPs than PCL and results in significant bone volume (Park et al., 2021b).

Aspirin is an anti-inflammatory and non-steroidal drug that inhibits osteoclast formation (by inhibiting the nuclear factor kappa-B pathway) and improves bone formation (by increasing the survival of bone marrow MSCs and stimulating the differentiation of preosteoblasts). Aspirin is effective on bone metabolism, and in low doses, it improves mineral density (Chin, 2017; Liu et al., 2022). The combination of aspirin and basic fetoprotein (BFP) in the PCL scaffold printed by Li et al. (Li et al., 2020b) improved osteogenic differentiation, bone remodeling, and the amount of new bone formation.

Platelet-rich plasma with various growth factors such as VEGF, platelet-derived growth factor (PDGF), and TGF- β improves the proliferation and differentiation of stem cells and bone repair. Li et al. (Li et al., 2017) coated the printed PCL scaffolds with platelet-rich plasma and enhanced the expression of RUNX2, osteocalcin, alkaline phosphatase, and osteopontin genes. The authors reported that these scaffolds improved bone formation and osteogenic differentiation.

The family of bisphosphonates, such as alendronate, are mainly nitrogen-containing drugs and play an essential role in osteoporosis treatment (Lieberman et al., 1995). Alendronate inhibits the synthesis of the substance needed to stimulate osteoclasts (geranylgeranyl pyrophosphate) and prevents bone resorption. In addition, improving the mechanical connection of the scaffold with the surrounding tissue accelerates bone healing (Tarafder and Bose, 2014; Kim S. E. et al., 2016). Alendronate increases the expression of BMP-2, osteocalcin, collagen, osteopontin, and alkaline phosphatase (Kim S. E. et al., 2016). Kim et al. (Kim S. E. et al., 2016) printed PCL/alendronate scaffolds, and reported that the sustained-alendronate release increased alkaline phosphatase activity, mineralization, and bone formation.

Shao et al. (Shao et al., 2019a) printed the PCL/Ag₃PO₄/lidocaine composite to benefit from the antibacterial effects of Ag₃PO₄ and lidocaine as an analgesic. Their results showed that it is possible to control the release of lidocaine by changing the diameter of the printed PCL filaments, so that it reaches the therapeutic effect within 4–7 days. In addition, by changing the amount of Ag₃PO₄-loading, their release can be controlled, and a sufficient antibacterial level can be achieved in at least 6 days. Levofloxacin (an antibiotic)/PCL was printed by Pupp et al. (Puppi et al., 2016b) to prevent the infectious complications associated with scaffold implantation with its controlled release. Their results showed a stable and uniform drug release profile during the 5 weeks.

6 Clinical applications

The controllability and unique properties of PCL, 3D printing technology, and the results of various animal models indicate the potential of this complex for clinical evaluations. This bioabsorbable polymer has been registered since 1980 and has resulted in potentially non-toxic products in diverse tissues (Moers-Carpi and Sherwood, 2013). Furthermore, PCL has been used in various clinical evaluations for bone tissue repair (available: <https://beta.clinicaltrials.gov/>). Clinical trials are conducted according to “good clinical practice” (GCP) standards in 3 phases. The product’s safety and effectiveness are evaluated on a small number of patients in the phases I and II, respectively. And the phase III, with the increase in the number of patients and the confirmation of the product’s effectiveness, began its

commercialization process (de Vries et al., 2008; Hollister and Murphy, 2011). The selection of patients for clinical trials should be done according to a specific protocol to be approved by regulatory centers and to reduce the influence of various factors on the results. Patient safety must be prioritized at all stages and must not pose a severe risk to the patient (Kleiderman et al., 2018; Kumar Gupta et al., 2022).

In a clinical trial, PCL was used to help improve and prevent the reduction of alveolar ridge height after tooth extraction, because the reduction of alveolar ridge height and volume prevents implant placement. This clinical evaluation was performed on 13 patients in two control groups (without scaffold) and the group with PCL scaffold immediately after tooth extraction. The width and height of the alveolar ridge were investigated 6 months after tooth extraction. Their results showed that the PCL scaffold improved bone healing and the maintenance of ridge height after 6 months (Tin Goh et al., 2014).

In another clinical trial, printed PCL scaffolds were used to repair caudal septal deviations. These printed scaffolds were used in 20 patients undergoing septoplasty, and the patients were followed up for 12 weeks. Their results showed that PCL scaffolds had favorable mechanical properties, biocompatibility, and ease of surgical manipulation. In addition, the presence of scaffold improves the Nasal Obstruction Symptom Evaluation score, the minimum cross-sectional area and the volume of the nasal cavity changes, and the nasal septum angle changes (Yun et al., 2018). In addition, PCL impregnated with Platelet-rich fibrin (PRF) has been used for ten outpatients with insufficient alveolar bone height around dental implants. Patients were follow-up for 3 months. Their results showed that this combination helped repair bone defects around dental implants and increase bone volume. In addition, no side effects (implant movement, pain, or infection) were observed after 3 months (Verma et al., 2014). Interbody fusion cage for the lumbar spinal stenosis treatment is another case that has used 3D printed PCL/TCP for clinical evaluations. In Xijing Hospital, 22 volunteer patients aged between 30 and 85 years underwent posterior lumbar interbody fusion surgery with PCL/TCP cages and were follow-up for 12 months. Their results showed that this cage increased bone fusion by 95.2%. And a significant improvement in clinical results was observed. Of course, entering the clinic requires longer evaluations and more patients (Liu et al., 2023). Other clinical trials have also used PCL for bone repair; some of these are mentioned in Table 3. However, it is necessary to mention that bed-to bedside translation of these products requires overcoming problems related to ethical issues, cost, regulatory rules, and ease of use by physicians (Hollister and Murphy, 2011).

The biggest challenges of the 3D printed PCL-based scaffolds to transfer to the bedside included the cost of printers, materials, and pre- and post-processing operations. These costs must be at least equivalent to current expensive treatments for scaffolds to be commercially viable. Although the cost of 3D printers has decreased significantly in recent years, it is still expensive for many medical centers. In addition, the cost of 3D printing materials is often higher than that of traditional methods (Li et al., 2015).

The lack of trained personnel is another challenges of transferring 3D printers to the bedside. Although the technology is becoming more user-friendly, it still requires trained professionals who can work with printers and design patient-specific scaffolds. In addition, the lack of accurate knowledge among doctors about this process and the lack of detailed studies on the effectiveness and safety of these products have led to the fact that doctors are more

TABLE 3 Clinical trials performed with PCL scaffolds for bone repair (database, 2018).

Composition	Indication	Clinical phase	Location
PCL	Orbital Fractures	Phase 2	Singapore/2004
3D-Printed PCL	Cranioplasty	Not Applicable	Singapore/2006
PCL/PRP/rhBMP-2	anterior mandible defect	Not Applicable	Germany/2009
PCL/TCP	Orbital walls	Phase 2	Singapore/2010
PCL	Nasal Septal Deformities	Not Applicable	Korea/2016
PCL mesh	orbital floor fracture	Not Applicable	Singapore/2017
3D Printed PCL-TCP	Ridge Preservation After Tooth Extraction	Not Applicable	Singapore/2019
Bone Marrow Aspirate Concentrate+3D-Printed PCL	Alveolar Defects	Not Applicable	Egypt/2022
3D-Printed PCL	pectus excavatum defects	Not Applicable	Australia/2022
PCL/PRF	Increasing bone volume and quality for dental implant implantation	Phase 1	India/2014
3D Printed PCL-TCP	lumbar interbody cage	Not Applicable	China/2023
PCL membrane	guided bone regeneration	Not Applicable	Thai/2020

inclined to use traditional methods. Close communication between clinicians and researchers will help accelerate the translation of this approach to the clinic (Hollister and Murphy, 2011). Furthermore, new technology such as, machine learning is a subset of artificial intelligence, which in recent years, with the help of 3D printing, has significantly reduced the time, cost, and effort required to design patient-specific models from imaging data (Huff et al., 2018).

Regulatory issues will also play an important role in the future evolution of 3D-printed PCL-based scaffolds at the bedside. Because 3D printing is a relatively new technology, guidelines for evaluating the safety and efficacy of 3D printed scaffolds are constantly evolving (Li et al., 2015). The FDA actively tracks the clinical 3D printing industry and has published precise guidelines for 3D printer manufacturers. There are several regulatory challenges for 3D-printed PCL-based scaffolds (especially cell-containing scaffolds). Generally, scaffolds without cells are known as class II medical devices, and scaffolds containing cells are known as class III medical devices in the guidelines, each of them requires compliance with certain standards and controls. Therefore, it is necessary to provide a specific regulatory path and standards to ensure the safety and reproducibility of 3D-printed PCL-based scaffolds (Li et al., 2015; Rahman et al., 2018; Bliley et al., 2022).

Although there are standards such as ISO/DIS 17296–1 for 3D printing terminology and 3D printer manufacturers, there is currently no specific standard for 3D bioprinting technology and inks (ISO, 2012). The level of standardization of inks and process is effective on the product development time and accelerates the clinical translation of the product, controls its quality, and reduces costs. In fact, with standardization, the manufacturers can optimize the printing method and ink composition and minimize the resources needed to make the product (Murphy et al., 2020; Jin et al., 2022).

Logistics requirements are another challenge in the clinical transfer of these products. Especially scaffolds containing cells are environmentally and time sensitive and require the design of a central logistics chain to ensure data collection and transplant tissue production. The patient-derived cells and materials must be

transported to a center, and the printed scaffolds returned to the patient (Murphy et al., 2020).

7 Conclusion and future perspectives

PCL, a thermoplastic and biodegradable polymer with unique mechanical properties and a slow degradation rate, is a potential biomaterial for the fabrication of BTE scaffolds. The compatibility of this polymer with 3D printing technology provides the patient-specific scaffolds with the desired size, shape, porosity, chemical composition, and suitable dimensions for the target tissue. Considering the better performance of PCL composite scaffolds compared to pure PCL, recent studies have used the combination of various ceramic, polymer, and metal materials with PCL to make bone tissue engineering scaffolds. The integration of these materials improves the properties of cell adhesion, degradability, osteoinductivity, and angiogenesis of the composite and helps to accelerate bone healing. In addition, various studies have also used the integration of drugs and growth factors to improve osteogenesis and angiogenesis in these scaffolds. 3D printing technology can integrate cells into PCL composite scaffolds. PCL composite scaffolds have been used in limited clinical trials to repair alveolar, orbital walls, and nasal septal defects, which indicates the potential of these composites for future applications. Of course, most of these trials are in their initial phases. Therefore, more clinical trials should be conducted for the design, implementation, and scalability of these composites. Integrating 3D printing technology with PCL composites soon will make it possible to create customized composite scaffolds containing the patient's cells by better mimicking bone architecture to aid in faster bone healing.

Author contributions

MG: Conceptualization, formal analysis, methodology, resources, writing—original draft. MS: Conceptualization,

formal analysis, methodology, writing—original draft. NB: visualization, Conceptualization, writing—original draft. MK-F: resources, writing—original draft. AA: resources, writing—original draft. M-SN: resources, writing—original draft. MA: Conceptualization, investigation, project administration, supervision, writing—original draft. All of the authors have read and approved the paper.

Acknowledgments

This study was supported as a part of PhD thesis (research NO.14010015) from Shahroud University of Medical Sciences.

References

- Ahn, T.-K., Lee, D. H., Kim, T. S., Jang, G. C., Choi, S., Oh, J. B., et al. (2018). Modification of titanium implant and titanium dioxide for bone tissue engineering. *Nov. Biomaterials Regen. Med.* 1077, 355–368. doi:10.1007/978-981-13-0947-2_19
- Arealis, G., and Nikolaou, V. S. (2015). Bone printing: New frontiers in the treatment of bone defects. *Injury* 46, S20–S22. doi:10.1016/s0020-1383(15)30050-4
- Asm International, D. L. B. e., and Frazier, W. (2020). “Additive manufacturing processes,” in *ASM handbook*. Editors Howard Kuhn and Mohsen Seifi (Tama: ASM International).
- Azarudeen, R. S., Hassan, M. N., Yassin, M. A., Thirumarimurugan, M., Muthukumarasamy, N., Velauthapillai, D., et al. (2020). 3D printable Polycaprolactone-gelatin blends characterized for *in vitro* osteogenic potency. *React. Funct. Polym.* 146, 104445. doi:10.1016/j.reactfunctpolym.2019.104445
- Bae, E.-B., Park, K. H., Shim, J. H., Chung, H. Y., Choi, J. W., Lee, J. J., et al. (2018b). Efficacy of rhBMP-2 loaded PCL/β-TCP/bdECM scaffold fabricated by 3D printing technology on bone regeneration. *BioMed Res. Int.* 2018, 1–12. doi:10.1155/2018/2876135
- Bae, E. B., Park, K. H., Shim, J. H., Chung, H. Y., Choi, J. W., Lee, J. J., et al. (2018a). Efficacy of rhBMP-2 loaded PCL/β-TCP/bdECM scaffold fabricated by 3D printing technology on bone regeneration. *Biomed. Res. Int.* 2018, 1–12. doi:10.1155/2018/2876135
- Bai, J., Wang, H., Gao, W., Liang, F., Wang, Z., Zhou, Y., et al. (2020). Melt electrohydrodynamic 3D printed poly (ε-caprolactone)/polyethylene glycol/roxithromycin scaffold as a potential anti-infective implant in bone repair. *Int. J. Pharm.* 576, 118941. doi:10.1016/j.ijpharm.2019.118941
- Beederman, M., Lamplot, J. D., Nan, G., Wang, J., Liu, X., Yin, L., et al. (2013). BMP signaling in mesenchymal stem cell differentiation and bone formation. *J. Biomed. Sci. Eng.* 6, 32–52. doi:10.4236/jbise.2013.68a1004
- Beheshtizadeh, N., Asgari, Y., Nasiri, N., Farzin, A., Ghorbani, M., Lotfikhshahiesh, N., et al. (2021). A network analysis of angiogenesis/osteogenesis-related growth factors in bone tissue engineering based on *in-vitro* and *in-vivo* data: A systems biology approach. *Tissue Cell* 72, 101553. doi:10.1016/j.tice.2021.101553
- Beheshtizadeh, N., Gharibshahian, M., Pazhouhnia, Z., Rostami, M., Zangi, A. R., Maleki, R., et al. (2022). Commercialization and regulation of regenerative medicine products: Promises, advances and challenges. *Biomed. Pharmacother.* 153, 113431. doi:10.1016/j.biopha.2022.113431
- Beheshtizadeh, N., Lotfikhshahiesh, N., Pazhouhnia, Z., Hoseinpour, M., and Nafari, M. (2020). A review of 3D bio-printing for bone and skin tissue engineering: A commercial approach. *J. Mater. Sci.* 55 (9), 3729–3749. doi:10.1007/s10853-019-04259-0
- Bharadwaz, A., and Jayasuriya, A. C. (2020). Recent trends in the application of widely used natural and synthetic polymer nanocomposites in bone tissue regeneration. *Mater. Sci. Eng. C Mater. Biol. Appl.* 110, 110698. doi:10.1016/j.msec.2020.110698
- Bikuna-Izagirre, M., Aldazabal, J., and Paredes, J. (2022). Gelatin blends enhance performance of electrospun polymeric scaffolds in comparison to coating protocols. *Polymers* 14 (7), 1311. doi:10.3390/polym14071311
- Biscaia, S., Branquinho, M. V., Alvites, R. D., Fonseca, R., Catarina Sousa, A., Pedrosa, S. S., et al. (2022a). 3D printed poly (?-Caprolactone)/Hydroxyapatite scaffolds for bone tissue engineering: A comparative study on composite preparation by melt blending or solvent casting techniques and influence of bioceramic content on scaffold properties. *Int. J. Mol. Sci.* 23, 2318. doi:10.3390/ijms23042318
- Biscaia, S., Pires, C., Livero, F. A. R., Bellan, D. L., Bini, I., Bustos, S. O., et al. (2022b). MG-pe: A novel Galectin-3 Ligand with antimelanoma properties and adjuvant effects to dacarbazine. *Int. J. Mol. Sci.* 23 (4), 7635. doi:10.3390/ijms23147635

Conflict of interest

The authors declare that the research was conducted in the absence of any commercial or financial relationships that could be construed as a potential conflict of interest.

Publisher's note

All claims expressed in this article are solely those of the authors and do not necessarily represent those of their affiliated organizations, or those of the publisher, the editors and the reviewers. Any product that may be evaluated in this article, or claim that may be made by its manufacturer, is not guaranteed or endorsed by the publisher.

Bliley, J. M., Shiwarski, D. J., and Feinberg, A. W. (2022). 3D-bioprinted human tissue and the path toward clinical translation. *Sci. Transl. Med.* 14 (666), eabo7047. doi:10.1126/scitranslmed.abo7047

Bolander, M. E., and Balian, G. (1986). The use of demineralized bone matrix in the repair of segmental defects. Augmentation with extracted matrix proteins and a comparison with autologous grafts. *J. Bone Jt. Surg. Am.* 68 (8), 1264–1274. doi:10.2106/00004623-198668080-00018

Borkar, T., Goenka, V., and Jaiswal, A. K. (2021). Application of poly-ε-caprolactone in extrusion-based bioprinting. *Bioprinting* 21, e00111. doi:10.1016/j.bprint.2020.e00111

Boschetto, A., and Bottini, L. (2014). Accuracy prediction in fused deposition modeling. *Int. J. Adv. Manuf. Technol.* 73 (5), 913–928. doi:10.1007/s00170-014-5886-4

Bruyas, A., Lou, F., Stahl, A. M., Gardner, M., Maloney, W., Goodman, S., et al. (2018a). Systematic characterization of 3D-printed PCL/β-TCP scaffolds for biomedical devices and bone tissue engineering: Influence of composition and porosity. *J. Mater. Res.* 33 (14), 1948–1959. doi:10.1557/jmr.2018.112

Bruyas, A., Lou, F., Stahl, A. M., Gardner, M., Maloney, W., Goodman, S., et al. (2018b). Systematic characterization of 3D-printed PCL/β-TCP scaffolds for biomedical devices and bone tissue engineering: Influence of composition and porosity. *J. Mater. Res.* 33 (14), 1948–1959. doi:10.1557/jmr.2018.112

Burg, K. J., Porter, S., and Kellam, J. F. (2000). Biomaterial developments for bone tissue engineering. *Biomaterials* 21 (23), 2347–2359. doi:10.1016/s0142-9612(00)0102-2

Buyuksungur, S., Hasirci, V., and Hasirci, N. (2021a). 3D printed hybrid bone constructs of PCL and dental pulp stem cells loaded GelMA. *J. Biomed. Mater. Res. Part A* 109 (12), 2425–2437. doi:10.1002/jbm.a.37235

Buyuksungur, S., Hasirci, V., and Hasirci, N. (2021b). 3D printed hybrid bone constructs of PCL and dental pulp stem cells loaded GelMA. *J. Biomed. Mater. Res. Part A* 109 (12), 2425–2437. doi:10.1002/jbm.a.37235

Cakmak, A. M., Unal, S., Sahin, A., Oktar, F. N., Sengor, M., Ekren, N., et al. (2020). 3D printed polycaprolactone/gelatin/bacterial cellulose/hydroxyapatite composite scaffold for bone tissue engineering. *Polymers* 12 (9), 1962. doi:10.3390/polym12091962

Campana, V., Milano, G., Pagano, E., Barba, M., Cicione, C., Salonna, G., et al. (2014). Bone substitutes in orthopaedic surgery: From basic science to clinical practice. *J. Mater. Sci. Mater. Med.* 25 (10), 2445–2461. doi:10.1007/s10856-014-5240-2

Cao, C., Huang, P., Prasopthum, A., Parsons, A. J., Ai, F., and Yang, J. (2022). Characterisation of bone regeneration in 3D printed ductile PCL/PEG/hydroxyapatite scaffolds with high ceramic microparticle concentrations. *Biomaterials Sci.* 10 (1), 138–152. doi:10.1039/d1bm01645h

Carano, R. A., and Filvaroff, E. H. (2003). Angiogenesis and bone repair. *Drug Discov. today* 8 (21), 980–989. doi:10.1016/s1359-6446(03)02866-6

Celikkin, N., Mastrogiacomo, S., Dou, W., Heerschap, A., Oosterwijk, E., Walboomers, X. F., et al. (2022). *In vitro* and *in vivo* assessment of a 3D printable gelatin methacrylate hydrogel for bone regeneration applications. *J. Biomed. Mater. Res. Part B Appl. Biomater.* 110, 2133–2145. doi:10.1002/jbm.b.35067

Chen, G., Zhou, P., Mei, N., Chen, X., Shao, Z., Pan*, L., et al. (2004). Silk fibroin modified porous poly (ε-caprolactone) scaffold for human fibroblast culture *in vitro*. *J. Mater. Sci. Mater. Med.* 15 (6), 671–677. doi:10.1023/b:jmsm.0000030208.89523.2a

Chen, S., Shi, Y., Zhang, X., and Ma, J. (2020). Evaluation of BMP-2 and VEGF loaded 3D printed hydroxyapatite composite scaffolds with enhanced osteogenic

- capacity *in vitro* and *in vivo*. *Mater. Sci. Eng. C* 112, 110893. doi:10.1016/j.msec.2020.110893
- Chin, K. Y. (2017). A review on the relationship between aspirin and bone health. *J. Osteoporos.* 2017, 1–8. doi:10.1155/2017/3710959
- Ciosek, Z., Kot, K., Kosik-Bogacka, D., Łanocha-Arendarczyk, N., and Rotter, I. (2021). The effects of calcium, magnesium, phosphorus, fluoride, and lead on bone tissue. *Biomolecules* 11 (4), 506. doi:10.3390/biom11040506
- Cox, S. C., Thornby, J. A., Gibbons, G. J., Williams, M. A., and Mallick, K. K. (2015). 3D printing of porous hydroxyapatite scaffolds intended for use in bone tissue engineering applications. *Mater. Sci. Eng. C* 47, 237–247. doi:10.1016/j.msec.2014.11.024
- Cunniffe, G. M., Gonzalez-Fernandez, T., Daly, A., Sathy, B. N., Jeon, O., Alsberg, E., et al. (2017). Three-Dimensional bioprinting of polycaprolactone reinforced gene activated bioinks for bone tissue engineering. *Tissue Eng. Part A* 23 (17–18), 891–900. doi:10.1089/ten.tea.2016.0498
- database, U. C. T. 2018 USA clinical trials database. Available from: <http://clinicaltrials.gov>.
- de Vries, R. B., Oerlemans, A., Trommelmans, L., Dierickx, K., and Gordijn, B. (2008). Ethical aspects of tissue engineering: A review. *Tissue Eng. Part B Rev.* 14 (4), 367–375. doi:10.1089/ten.teb.2008.0199
- Dong, L., Wang, S. J., Zhao, X. R., Zhu, Y. F., and Yu, J. K. (2017). 3D-printed poly(ϵ -caprolactone) scaffold integrated with cell-laden chitosan hydrogels for bone tissue engineering. *Sci. Rep.* 7 (1), 13412. doi:10.1038/s41598-017-13838-7
- Dong, Q., Zhang, M., Zhou, X., Shao, Y., Li, J., Wang, L., et al. (2021). 3D-printed Mg-incorporated PCL-based scaffolds: A promising approach for bone healing. *Mater. Sci. Eng. C* 129, 112372. doi:10.1016/j.msec.2021.112372
- Doyle, H., Lohfeld, S., and McHugh, P. (2015). Evaluating the effect of increasing ceramic content on the mechanical properties, material microstructure and degradation of selective laser sintered polycaprolactone/ β -tricalcium phosphate materials. *Med. Eng. Phys.* 37 (8), 767–776. doi:10.1016/j.medengphy.2015.05.009
- Du, X., Wei, D., Huang, L., Zhu, M., Zhang, Y., and Zhu, Y. (2019). 3D printing of mesoporous bioactive glass/silk fibroin composite scaffolds for bone tissue engineering. *Mater. Sci. Eng. C* 103, 109731. doi:10.1016/j.msec.2019.05.016
- Duan, M., Ma, S., Song, C., Li, J., and Qian, M. (2021). Three-dimensional printing of a β -tricalcium phosphate scaffold with dual bioactivities for bone repair. *Ceram. Int.* 47 (4), 4775–4782. doi:10.1016/j.ceramint.2020.10.047
- Duyamaz, B. T., Erdiler, F. B., Alan, T., Aydogdu, M. O., Inan, A. T., Ekren, N., et al. (2019). 3D bio-printing of levan/polycaprolactone/gelatin blends for bone tissue engineering: Characterization of the cellular behavior. *Eur. Polym. J.* 119, 426–437. doi:10.1016/j.eurpolymj.2019.08.015
- El-Habashy, S. E., El-Kamel, A. H., Essawy, M. M., Abdelfattah, E. Z. A., and Eltahir, H. M. (2021). Engineering 3D-printed core-shell hydrogel scaffolds reinforced with hybrid hydroxyapatite/polycaprolactone nanoparticles for *in vivo* bone regeneration. *Biomaterials Sci.* 9 (11), 4019–4039. doi:10.1039/d1bm00062d
- Elomaa, L., Kokkari, A., Närhi, T., and Seppälä, J. (2011a). Porous polycaprolactone/bioactive glass scaffold prepared by stereolithography. *Eur. Conf. Biomaterials.*
- Elomaa, L., Keshi, E., Sauer, I. M., and Weinhart, M. (2020). Development of GelMA/PCL and dECM/PCL resins for 3D printing of acellular *in vitro* tissue scaffolds by stereolithography. *Mater. Sci. Eng. C* 112, 110958. doi:10.1016/j.msec.2020.110958
- Elomaa, L., Teixeira, S., Hakala, R., Korhonen, H., Grijpma, D. W., and Seppälä, J. V. (2011b). Preparation of poly(ϵ -caprolactone)-based tissue engineering scaffolds by stereolithography. *Acta Biomater.* 7 (11), 3850–3856. doi:10.1016/j.actbio.2011.06.039
- Eosoly, S., Vrana, N. E., Lohfeld, S., Hindie, M., and Looney, L. (2012). Interaction of cell culture with composition effects on the mechanical properties of polycaprolactone-hydroxyapatite scaffolds fabricated via selective laser sintering (SLS). *Mater. Sci. Eng. C* 32 (8), 2250–2257. doi:10.1016/j.msec.2012.06.011
- Erbe, E. J., M., T., C., and L., B. (2001). Potential of an ultraporous β -tricalcium phosphate synthetic cancellous bone void filler and bone marrow aspirate composite graft. *Eur. Spine J.* 10 (2), S141–S146. doi:10.1007/s005860100287
- Fallah, A., Altunbek, M., Bartolo, P., Cooper, G., Weightman, A., Blunn, G., et al. (2022). 3D printed scaffold design for bone defects with improved mechanical and biological properties. *J. Mech. Behav. Biomed. Mater.* 134, 105418. doi:10.1016/j.jmbm.2022.105418
- Farid, S. B. H. (2019). *Bioceramics: For materials science and engineering*. Netherlands: Woodhead Publishing Series in Biomaterials.
- Farokhi, M., Mottaghtalab, F., Samani, S., Shokrgozar, M. A., Kundu, S. C., Reis, R. L., et al. (2018). Silk fibroin/hydroxyapatite composites for bone tissue engineering. *Biotechnol. Adv.* 36 (1), 68–91. doi:10.1016/j.biotechadv.2017.10.001
- Farzadi, A., Solati-Hashjin, M., Asadi-Eydivand, M., and Abu Osman, N. A. (2014). Effect of layer thickness and printing orientation on mechanical properties and dimensional accuracy of 3D printed porous samples for bone tissue engineering. *PLoS one* 9 (9), e108252. doi:10.1371/journal.pone.0108252
- Fathi, A., Kermani, F., Behnamghader, A., Banijamali, S., Mozafari, M., Baines, F., et al. (2020). Three-dimensionally printed polycaprolactone/multicomponent bioactive glass scaffolds for potential application in bone tissue engineering. *Biomed. Glas.* 6 (1), 57–69. doi:10.1515/bglass-2020-0006
- Fathi-Achachelouei, M., Knopf-Marques, H., Ribeiro da Silva, C. E., Barthès, J., Bat, E., Tezcaner, A., et al. (2019). Use of nanoparticles in tissue engineering and regenerative medicine. *Front. Bioeng. Biotechnol.* 7, 113. doi:10.3389/fbioe.2019.00113
- FDA (2006). *510K K051093 osteopore PCL scaffold bone void filler(BVF)*. Rockville, MD: FDA. Available from www.accessdata.fda.gov.
- Fleming, J. E., Cornell, C. N., and Muschler, G. F. (2000). Bone cells and matrices in orthopedic tissue engineering. *Orthop. Clin.* 31 (3), 357–374. doi:10.1016/s0030-5898(05)70156-5
- Galarraga, J. H., Kwon, M. Y., and Burdick, J. A. (2019). 3D bioprinting via an *in situ* crosslinking technique towards engineering cartilage tissue. *Sci. Rep.* 9 (1), 19987–19999. doi:10.1038/s41598-019-56117-3
- Gatto, M. L., Furlani, M., Giuliani, A., Bloise, N., Fassina, L., Visai, L., et al. (2021). Biomechanical performances of PCL/HA micro- and macro-porous lattice scaffolds fabricated via laser powder bed fusion for bone tissue engineering. *Mater. Sci. Eng. C Mater. Biol. Appl.* 128, 112300. doi:10.1016/j.msec.2021.112300
- Gautam, S., Sharma, C., Purohit, S. D., Singh, H., Dinda, A. K., Potdar, P. D., et al. (2021). Gelatin-polycaprolactone-nanohydroxyapatite electrospun nanocomposite scaffold for bone tissue engineering. *Mater. Sci. Eng. C* 119, 111588. doi:10.1016/j.msec.2020.111588
- Genova, T., Roato, I., Carossa, M., Motta, C., Cavagnetto, D., and Mussano, F. (2020). Advances on bone substitutes through 3D bioprinting. *Int. J. Mol. Sci.* 21 (19), 7012. doi:10.3390/ijms21197012
- Ghorbani, F. M., Kaffashi, B., Shokrollahi, P., Seyedjafari, E., and Ardeshtyrlajimi, A. (2015). PCL/chitosan/Zn-doped nHA electrospun nanocomposite scaffold promotes adipose derived stem cells adhesion and proliferation. *Carbohydr. Polym.* 118, 133–142. doi:10.1016/j.carbpol.2014.10.071
- Giuliani, A., Manescu, A., Mohammadi, S., Mazzoni, S., Piattelli, A., Mangano, F., et al. (2016). Quantitative kinetics evaluation of blocks versus granules of biphasic calcium phosphate scaffolds (HA/ β -TCP 30/70) by synchrotron radiation x-ray microtomography: A human study. *Implant Dent.* 25 (1), 6–15. doi:10.1097/id.0000000000000363
- Gonçalves, E. M., Oliveira, F. J., Silva, R. F., Neto, M. A., Fernandes, M. H., Amaral, M., et al. (2016). Three-dimensional printed PCL-hydroxyapatite scaffolds filled with CNTs for bone cell growth stimulation. *J. Biomed. Mater. Res. B Appl. Biomater.* 104 (6), 1210–1219. doi:10.1002/jbm.b.33432
- Goncalves, E. M., Oliveira, F. J., Silva, R. F., Neto, M. A., Fernandes, M. H., Amaral, M., et al. (2016). Three-dimensional printed PCL-hydroxyapatite scaffolds filled with CNTs for bone cell growth stimulation. *J. Biomed. Mater. Res. Part B Appl. Biomaterials* 104 (6), 1210–1219. doi:10.1002/jbm.b.33432
- Gong, B., Cui, S., Zhao, Y., Sun, Y., and Ding, Q. (2017). Strain-controlled fatigue behaviors of porous PLA-based scaffolds by 3D-printing technology. *J. Biomaterials Sci. Polym. Ed.* 28 (18), 2196–2204. doi:10.1080/09205063.2017.1388993
- Grémare, A., Guduric, V., Bareille, R., Heroguez, V., Latour, S., L'heureux, N., et al. (2018). Characterization of printed PLA scaffolds for bone tissue engineering. *J. Biomed. Mater. Res. Part A* 106 (4), 887–894. doi:10.1002/jbm.a.36289
- Haffner, M., Quinn, A., Hsieh, T. y., Strong, E. B., and Steele, T. (2018). Optimization of 3D print material for the recreation of patient-specific temporal bone models. *Ann. Otolaryngol. Rhinol. Laryngol.* 127 (5), 338–343. doi:10.1177/0003489418764987
- Han, H.-S., Loffredo, S., Jun, I., Edwards, J., Kim, Y. C., Seok, H. K., et al. (2019). Current status and outlook on the clinical translation of biodegradable metals. *Mater. Today* 23, 57–71. doi:10.1016/j.mattod.2018.05.018
- Hann, S. Y., Cui, H., Esworthy, T., Miao, S., Zhou, X., Lee, S. j., et al. (2019). Recent advances in 3D printing: Vascular network for tissue and organ regeneration. *Transl. Res.* 211, 46–63. doi:10.1016/j.trsl.2019.04.002
- Hassanajili, S., Karami-Pour, A., Oryan, A., and Talaei-Khozani, T. (2019a). Preparation and characterization of PLA/PCL/HA composite scaffolds using indirect 3D printing for bone tissue engineering. *Mater. Sci. Eng. C* 104, 109960. doi:10.1016/j.msec.2019.109960
- Hassanajili, S., Karami-Pour, A., Oryan, A., and Talaei-Khozani, T. (2019b). Preparation and characterization of PLA/PCL/HA composite scaffolds using indirect 3D printing for bone tissue engineering. *Mater. Sci. Eng. C Mater. Biol. Appl.* 104, 109960. doi:10.1016/j.msec.2019.109960
- He, Y. (2016). *An investigation of inkjet printing of polycaprolactone based inks*. England: University of Nottingham.
- He, Y., Tuck, C. J., Prina, E., Kilsby, S., Christie, S. D. R., Edmondson, S., et al. (2017). A new photocrosslinkable polycaprolactone-based ink for three-dimensional inkjet printing. *J. Biomed. Mater. Res. Part B Appl. Biomaterials* 105 (6), 1645–1657. doi:10.1002/jbm.b.33699
- Heo, E. Y., Ko, N. R., Bae, M. S., Lee, S. J., Choi, B. J., Kim, J. H., et al. (2017). Novel 3D printed alginate-BFP1 hybrid scaffolds for enhanced bone regeneration. *J. Industrial Eng. Chem.* 45, 61–67. doi:10.1016/j.jiec.2016.09.003

- Heo, S. Y., Ko, S. C., Nam, S. Y., Oh, J., Kim, Y. M., Kim, J. I., et al. (2018). Fish bone peptide promotes osteogenic differentiation of MC3T3-E1 pre-osteoblasts through upregulation of MAPKs and Smad pathways activated BMP-2 receptor. *Cell Biochem. Funct.* 36 (3), 137–146. doi:10.1002/cbf.3325
- Heo, S. Y., Ko, S., Oh, G., Kim, N., Choi, I., Park, W. S., et al. (2019b). Fabrication and characterization of the 3D-printed polycaprolactone/fish bone extract scaffolds for bone tissue regeneration. *J. Biomed. Mater. Res. B Appl. Biomater.* 107 (6), 1937–1944. doi:10.1002/jbm.b.34286
- Heo, S. Y., Ko, S., Oh, G., Kim, N., Choi, I., Park, W. S., et al. (2019a). Fabrication and characterization of the 3D-printed polycaprolactone/fish bone extract scaffolds for bone tissue regeneration. *J. Biomed. Mater. Res. Part B Appl. Biomaterials* 107 (6), 1937–1944. doi:10.1002/jbm.b.34286
- Hernandez, I., Kumar, A., and Joddar, B. (2017a). A bioactive hydrogel and 3D printed polycaprolactone system for bone tissue engineering. *Gels* 3 (3), 26. doi:10.3390/gels3030026
- Hernandez, I., Kumar, A., and Joddar, B. (2017b). A bioactive hydrogel and 3D printed polycaprolactone system for bone tissue engineering. *Gels* 3 (3), 26. doi:10.3390/gels3030026
- Hollister, S. J., and Murphy, W. L. (2011). Scaffold translation: Barriers between concept and clinic. *Tissue Eng. Part B Rev.* 17 (6), 459–474. doi:10.1089/ten.teb.2011.0251
- Huang, B., Caetano, G., Vyas, C., Blaker, J., Diver, C., and Bártolo, P. (2018). Polymer-ceramic composite scaffolds: The effect of hydroxyapatite and β -tri-calcium phosphate. *Mater. (Basel)* 11 (1), 129. doi:10.3390/ma11010129
- Huber, F., Vollmer, D., Vinke, J., Riedel, B., Zankovic, S., Schmal, H., et al. (2022). Influence of 3D printing parameters on the mechanical stability of PCL scaffolds and the proliferation behavior of bone cells. *Materials* 15 (6), 2091. doi:10.3390/ma15062091
- Huff, T. J., Ludwig, P. E., and Zuniga, J. M. (2018). The potential for machine learning algorithms to improve and reduce the cost of 3-dimensional printing for surgical planning. *Expert Rev. Med. devices* 15 (5), 349–356. doi:10.1080/17434440.2018.1473033
- Hwang, K.-S., Choi, J. W., Kim, J. H., Chung, H., Jin, S., Shim, J. H., et al. (2017a). Comparative efficacies of collagen-based 3D printed PCL/PLGA/ β -TCP composite block bone grafts and biphasic calcium phosphate bone substitute for bone regeneration. *Materials* 10 (4), 421. doi:10.3390/ma10040421
- Hwang, K. S., Choi, J. W., Kim, J. H., Chung, H., Jin, S., Shim, J. H., et al. (2017b). Comparative efficacies of collagen-based 3D printed PCL/PLGA/ β -TCP composite block bone grafts and biphasic calcium phosphate bone substitute for bone regeneration. *Mater. (Basel)* 10 (4), 421. doi:10.3390/ma10040421
- ISO 1212 ISO/DIS 17296-1(en). *Additive manufacturing — general principles — Part 1: Terminology*.
- Jin, Z., Fu, J., Han, Q., and He, Y. (2022). Balancing the customization and standardization: Exploration and layout surrounding the regulation of the growing field of 3D-printed medical devices in China. *Bio-design Manuf.* 5 (3), 580–606. doi:10.1007/s42242-022-00187-2
- Jonathan Black, G. H. (1998). *Handbook of biomaterial properties*. Germany: Springer.
- Karageorgiou, V., and Kaplan, D. (2005). Porosity of 3D biomaterial scaffolds and osteogenesis. *Biomaterials* 26 (27), 5474–5491. doi:10.1016/j.biomaterials.2005.02.002
- Karimzadeh Bardeei, L., Seyedjafari, E., Hossein, G., Nabiuni, M., Majles Ara, M. H., and Salber, J. (2021). Regeneration of bone defects in a rabbit femoral osteonecrosis model using 3D-printed poly (Epsilon-Caprolactone)/Nanoparticulate willemite composite scaffolds. *Int. J. Mol. Sci.* 22 (19), 10332. doi:10.3390/ijms221910332
- Ke, D., Yu, J., Liu, P., Niu, C., and Yang, X. (2022). Biomimetic 3D printed PCL/TCP/GelMA scaffolds with improved osteogenesis and angiogenesis for non-load bearing applications. *Materialia* 21, 101339. doi:10.1016/j.mtl.2022.101339
- Keating, J. F., Simpson, A., and Robinson, C. (2005). The management of fractures with bone loss. *J. bone ft. Surg. Br. volume* 87 (2), 142–150. doi:10.1302/0301-620x.87b2.15874
- Kim, J. Y., Ahn, G., Kim, C., Lee, J. S., Lee, I. G., An, S. H., et al. (2018). Synergistic effects of beta tri-calcium phosphate and porcine-derived decellularized bone extracellular matrix in 3D-printed polycaprolactone scaffold on bone regeneration. *Macromol. Biosci.* 18 (6), 1800025. doi:10.1002/mabi.201800025
- Kim, S. E., Yun, Y. P., Shim, K. S., Kim, H. J., Park, K., and Song, H. R. (2016a). 3D printed alendronate-releasing poly (caprolactone) porous scaffolds enhance osteogenic differentiation and bone formation in rat tibial defects. *Biomed. Mater.* 11 (5), 055005. doi:10.1088/1748-6041/11/5/055005
- Kim, Y., Lee, S. H., Kang, B. j., Kim, W. H., Yun, H. s., and Kweon, O. k. (2016b). Comparison of osteogenesis between adipose-derived mesenchymal stem cells and their sheets on poly- ϵ -caprolactone/ β -tricalcium phosphate composite scaffolds in canine bone defects. *Stem Cells Int.* 2016, 1–10. doi:10.1155/2016/8414715
- Kleiderman, E., Boily, A., Hasilo, C., and Knoppers, B. M. (2018). Overcoming barriers to facilitate the regulation of multi-centre regenerative medicine clinical trials. *Stem Cell Res. Ther.* 9, 307–309. doi:10.1186/s13287-018-1055-2
- Koch, F., Thaden, O., Conrad, S., Tröndle, K., Finkenzeller, G., Zengerle, R., et al. (2022). Mechanical properties of polycaprolactone (PCL) scaffolds for hybrid 3D-bioprinting with alginate-gelatin hydrogel. *J. Mech. Behav. Biomed. Mater.* 130, 105219. doi:10.1016/j.jmbmm.2022.105219
- Konopnicki, S., Sharaf, B., Resnick, C., Patenaude, A., Pogal-Sussman, T., Hwang, K. G., et al. (2015). Tissue-engineered bone with 3-dimensionally printed β -tricalcium phosphate and polycaprolactone scaffolds and early implantation: An *in vivo* pilot study in a porcine mandible model. *J. Oral Maxillofac. Surg.* 73 (5), 1016. e1–e1016.e11. doi:10.1016/j.joms.2015.01.021
- Koons, G. L., Diba, M., and Mikos, A. G. (2020). Materials design for bone-tissue engineering. *Nat. Rev. Mater.* 5 (8), 584–603. doi:10.1038/s41578-020-0204-2
- Ku, J., Kim, Y., and Um, I. (2015). The retrospective clinical study of the autogenous tooth block bone graft. *J. Dent. Implant. Res.* 34, 27–34.
- Kumar Gupta, D., Ali, M. H., Ali, A., Jain, P., Anwer, M. K., Iqbal, Z., et al. (2022). 3D printing technology in healthcare: Applications, regulatory understanding, IP repository and clinical trial status. *J. Drug Target.* 30 (2), 131–150. doi:10.1080/1061186x.2021.1935973
- Kyle, S., Jessop, Z. M., Al-Sabah, A., and Whitaker, I. S. (2017). Printability of candidate biomaterials for extrusion based 3D printing: State-of-the-art. *Adv. Healthc. Mater.* 6 (16), 1700264. doi:10.1002/adhm.201700264
- L Mescher, A. (2018). *Junqueira's basic histology text and atlas*. New York: McGraw-Hill Education. FIFTEENTH.
- Lanza, R., Langer, R., and Vacanti, J. (2020). *Principles of tissue engineering*. Cambridge: Academic Press.
- Laurent, S., Dutz, S., Häfeli, U. O., and Mahmoudi, M. (2011). Magnetic fluid hyperthermia: Focus on superparamagnetic iron oxide nanoparticles. *Adv. Colloid Interface Sci.* 166 (1–2), 8–23. doi:10.1016/j.cis.2011.04.003
- Lee, H., Yeo, M., Ahn, S., Kang, D. O., Jang, C. H., Lee, H., et al. (2011). Designed hybrid scaffolds consisting of polycaprolactone microstrands and electrospun collagen-nanofibers for bone tissue regeneration. *J. Biomed. Mater. Res. Part B Appl. biomaterials* 97 (2), 263–270. doi:10.1002/jbm.b.31809
- Lee, J.-H., Park, J. K., and Son, K. H. (2022). PCL/sodium-alginate based 3D-printed dual drug delivery system with antibacterial activity for osteomyelitis therapy. *Gels* 8 (3), 163. doi:10.3390/gels8030163
- Lei, B., Gao, X., Zhang, R., Yi, X., and Zhou, Q. (2022). *In situ* magnesium phosphate/polycaprolactone 3D-printed scaffold induce bone regeneration in rabbit maxillofacial bone defect model. *Mater. Des.* 215, 110477. doi:10.1016/j.matdes.2022.110477
- Li, G., Yang, H., Zheng, Y., Chen, X. H., Yang, J. A., Zhu, D., et al. (2019). Challenges in the use of zinc and its alloys as biodegradable metals: Perspective from biomechanical compatibility. *Acta Biomater.* 97, 23–45. doi:10.1016/j.actbio.2019.07.038
- Li, J., Chen, M., Wei, X., Hao, Y., and Wang, J. (2017). Evaluation of 3D-printed polycaprolactone scaffolds coated with freeze-dried platelet-rich plasma for bone regeneration. *Materials* 10 (7), 831. doi:10.3390/ma10070831
- Li, J., He, L., Zhou, C., Zhou, Y., Bai, Y., Lee, F. Y., et al. (2015). 3D printing for regenerative medicine: From bench to bedside. *Mrs Bull.* 40 (2), 145–154. doi:10.1557/mrs.2015.5
- Li, Y., Li, Q., Li, H., Xu, X., Fu, X., Pan, J., et al. (2020b). An effective dual-factor modified 3D-printed PCL scaffold for bone defect repair. *J. Biomed. Mater. Res. B Appl. Biomater.* 108 (5), 2167–2179. doi:10.1002/jbm.b.34555
- Li, Y., Li, Q., Li, H., Xu, X., Fu, X., Pan, J., et al. (2020a). An effective dual-factor modified 3D-printed PCL scaffold for bone defect repair. *J. Biomed. Mater. Res. Part B Appl. Biomaterials* 108 (5), 2167–2179. doi:10.1002/jbm.b.34555
- Liao, H. T., Lee, M. Y., Tsai, W. W., Wang, H. C., and Lu, W. C. (2016). Osteogenesis of adipose-derived stem cells on polycaprolactone- β -tricalcium phosphate scaffold fabricated via selective laser sintering and surface coating with collagen type I. *J. tissue Eng. Regen. Med.* 10 (10), E337–E353. doi:10.1002/term.1811
- Liberman, U. A., Weiss, S. R., Bröll, J., Minne, H. W., Quan, H., Bell, N. H., et al. (1995). Effect of oral alendronate on bone mineral density and the incidence of fractures in postmenopausal osteoporosis. *N. Engl. J. Med.* 333 (22), 1437–1444. doi:10.1056/nejm199511303332201
- Liu, D., Nie, W., Li, D., Wang, W., Zheng, L., Zhang, J., et al. (2019). 3D printed PCL/SrHA scaffold for enhanced bone regeneration. *Chem. Eng. J.* 362, 269–279. doi:10.1016/j.cej.2019.01.015
- Liu, H., Du, Y., Yang, G., Hu, X., Wang, L., Liu, B., et al. (2020c). Delivering proangiogenic factors from 3D-printed polycaprolactone scaffolds for vascularized bone regeneration. *Adv. Healthc. Mater.* 9, e2000727. doi:10.1002/adhm.202000727
- Liu, H., Du, Y., Yang, G., Hu, X., Wang, L., Liu, B., et al. (2020b). Delivering proangiogenic factors from 3D-printed polycaprolactone scaffolds for vascularized bone regeneration. *Adv. Healthc. Mater.* 9 (23), 2000727. doi:10.1002/adhm.202000727
- Liu, H., Xiao, X., Shi, Q., Tang, X., and Tian, Y. (2022). Low dose aspirin associated with greater bone mineral density in older adults. *Sci. Rep.* 12 (1), 14887. doi:10.1038/s41598-022-19315-0
- Liu, Y., Wang, R., Chen, S., Xu, Z., Wang, Q., Yuan, P., et al. (2020a). Heparan sulfate loaded polycaprolactone-hydroxyapatite scaffolds with 3D printing for bone defect repair. *Int. J. Biol. Macromol.* 148, 153–162. doi:10.1016/j.jbiomac.2020.01.109

- Liu, Y., Wu, H., Bao, S., Huang, H., Tang, Z., Dong, H., et al. (2023). Clinical application of 3D-printed biodegradable lumbar interbody cage (polycaprolactone/ β -tricalcium phosphate) for posterior lumbar interbody fusion. *J. Biomed. Mater. Res. Part B Appl. Biomaterials* 111, 1398–1406. doi:10.1002/jbm.b.35244
- Maleki-Ghaleh, H., Hossein Siadati, M., Fallah, A., Zarrabi, A., Afghah, F., Koc, B., et al. (2021). Effect of zinc-doped hydroxyapatite/graphene nanocomposite on the physicochemical properties and osteogenesis differentiation of 3D-printed polycaprolactone scaffolds for bone tissue engineering. *Chem. Eng. J.* 426, 131321. doi:10.1016/j.cej.2021.131321
- Malikmammadov, E., Tanir, T. E., Kiziltay, A., and Hasirci, N. (2019). Preparation and characterization of poly (ϵ -caprolactone) scaffolds modified with cell-loaded fibrin gel. *Int. J. Biol. Macromol.* 125, 683–689. doi:10.1016/j.ijbiomac.2018.12.036
- Malikmammadov, E., Tanir, T. E., Kiziltay, A., Hasirci, V., and Hasirci, N. (2018). PCL and PCL-based materials in biomedical applications. *J. Biomaterials Sci. Polym. Ed.* 29 (7–9), 863–893. doi:10.1080/09205063.2017.1394711
- Melchels, F. P., Feijen, J., and Grijpma, D. W. (2010). A review on stereolithography and its applications in biomedical engineering. *Biomaterials* 31 (24), 6121–6130. doi:10.1016/j.biomaterials.2010.04.050
- Metwally, S., Ferraris, S., Spriano, S., Krysiak, Z. J., Kaniuk, L., Marzec, M. M., et al. (2020). Surface potential and roughness controlled cell adhesion and collagen formation in electrospun PCL fibers for bone regeneration. *Mater. Des.* 194, 108915. doi:10.1016/j.matdes.2020.108915
- Middleton, J. C., and Tipton, A. J. (2000). Synthetic biodegradable polymers as orthopedic devices. *Biomaterials* 21 (23), 2335–2346. doi:10.1016/s0142-9612(00)00101-0
- Midha, S., Dalela, M., Sybil, D., Patra, P., and Mohanty, S. (2019). Advances in three-dimensional bioprinting of bone: Progress and challenges. *J. tissue Eng. Regen. Med.* 13 (6), term.2847–945. doi:10.1002/term.2847
- Modi, Y. K., and Sahu, K. K. (2021). Process parameter optimization for porosity and compressive strength of calcium sulfate based 3D printed porous bone scaffolds. *Rapid Prototyp. J.* 27, 245–255. doi:10.1108/rpj-04-2020-0083
- Moers-Carpi, M. M., and Sherwood, S. (2013). Polycaprolactone for the correction of nasolabial folds: A 24-month, prospective, randomized, controlled clinical trial. *Dermatol. Surg.* 39, 457–463. doi:10.1111/dsu.12054
- Mohamed, O. A., Masood, S. H., and Bhowmik, J. L. (2015). Optimization of fused deposition modeling process parameters: A review of current research and future prospects. *Adv. Manuf.* 3 (1), 42–53. doi:10.1007/s40436-014-0097-7
- Mondal, S., Nguyen, T. P., Pham, V. H., Hoang, G., Manivasagan, P., Kim, M. H., et al. (2020). Hydroxyapatite nano bioceramics optimized 3D printed poly lactic acid scaffold for bone tissue engineering application. *Ceram. Int.* 46 (3), 3443–3455. doi:10.1016/j.ceramint.2019.10.057
- Monfared, M. H., Nemati, A., Loghman, F., Ghasemian, M., Farzin, A., Beheshtizadeh, N., et al. (2022). A deep insight into the preparation of ceramic bone scaffolds utilizing robocasting technique. *Ceram. Int.* 48 (5), 5939–5954. doi:10.1016/j.ceramint.2021.11.268
- Müller, W. E., Tolba, E., Schröder, H. C., and Wang, X. (2015). Polyphosphate: A morphogenetically active implant material serving as metabolic fuel for bone regeneration. *Macromol. Biosci.* 15 (9), 1182–1197. doi:10.1002/mabi.201500100
- Murphy, C., Kolan, K., Li, W., Semon, J., Day, D., and Leu, M. (2017a). 3D bioprinting of stem cells and polymer/bioactive glass composite scaffolds for bone tissue engineering. *Int. J. Bioprinting* 3 (1), 005. doi:10.18063/ijb.2017.01.005
- Murphy, C., Kolan, K., Li, W., Semon, J., Day, D., and Leu, M. (2017b). 3D bioprinting of stem cells and polymer/bioactive glass composite scaffolds for bone tissue engineering. *Int. J. Bioprint* 3 (1), 005. doi:10.18063/IJB.2017.01.005
- Murphy, S. V., and Atala, A. (2014). 3D bioprinting of tissues and organs. *Nat. Biotechnol.* 32 (8), 773–785. doi:10.1038/nbt.2958
- Murphy, S. V., De Coppi, P., and Atala, A. (2020). Opportunities and challenges of translational 3D bioprinting. *Nat. Biomed. Eng.* 4 (4), 370–380. doi:10.1038/s41551-019-0471-7
- Neufurth, M., Wang, X., Wang, S., Steffen, R., Ackermann, M., Haep, N. D., et al. (2017). 3D printing of hybrid biomaterials for bone tissue engineering: Calcium-polyphosphate microparticles encapsulated by polycaprolactone. *Acta Biomater.* 64, 377–388. doi:10.1016/j.actbio.2017.09.031
- Niyogi, S., Bekyarova, E., Itkis, M. E., McWilliams, J. L., Hamon, M. A., and Haddon, R. C. (2006). Solution properties of graphite and graphene. *J. Am. Chem. Soc.* 128 (24), 7720–7721. doi:10.1021/ja060680r
- Park, H., Kim, J. S., Oh, E. J., Kim, T. J., Kim, H. M., Shim, J. H., et al. (2018a). Effects of three-dimensionally printed polycaprolactone/ β -tricalcium phosphate scaffold on osteogenic differentiation of adipose tissue- and bone marrow-derived stem cells. *Archives Craniofacial Surg.* 19 (3), 181–189. doi:10.7181/acfs.2018.01879
- Park, S. A., Lee, H., Kim, S., Kim, K., and Jo, D. (2021b). Three-dimensionally printed polycaprolactone/ β -tricalcium phosphate scaffold was more effective as an rhBMP-2 carrier for new bone formation than polycaprolactone alone. *J. Biomed. Mater. Res. A* 109 (6), 840–848. doi:10.1002/jbm.a.37075
- Park, S. A., Lee, H., Kim, S., Kim, K., and Jo, D. (2021a). Three-dimensionally printed polycaprolactone/ β -tricalcium phosphate scaffold was more effective as an rhBMP-2 carrier for new bone formation than polycaprolactone alone. *J. Biomed. Mater. Res. Part A* 109 (6), 840–848. doi:10.1002/jbm.a.37075
- Park, S. A., Lee, S. J., Seok, J. M., Lee, J. H., Kim, W. D., and Kwon, I. K. (2018b). Fabrication of 3D printed PCL/PEG polyblend scaffold using rapid prototyping system for bone tissue engineering application. *J. Bionic Eng.* 15 (3), 435–442. doi:10.1007/s42235-018-0034-8
- Partee, B., Hollister, S. J., and Das, S. (2006). Selective laser sintering process optimization for layered manufacturing of CAPA[®] 6501 polycaprolactone bone tissue engineering scaffolds. *J. Manuf. Sci. Eng.* 128.
- Pati, F., Jang, J., Lee, J. W., and Cho, D. W. (2015a). “Extrusion bioprinting,” in *Essentials of 3D biofabrication and translation* (Netherlands: Elsevier).
- Pati, F., Jang, J., Ha, D. H., Won Kim, S., Rhie, J. W., Shim, J. H., et al. (2014). Printing three-dimensional tissue analogues with decellularized extracellular matrix bioink. *Nat. Commun.* 5, 3935. doi:10.1038/ncomms4935
- Pati, F., Song, T. H., Rijal, G., Jang, J., Kim, S. W., and Cho, D. W. (2015b). Ornamenting 3D printed scaffolds with cell-laid extracellular matrix for bone tissue regeneration. *Biomaterials* 37, 230–241. doi:10.1016/j.biomaterials.2014.10.012
- Pattanashetti, N. A., Biscaia, S., Moura, C., Mitchell, G. R., and Kariduraganavar, M. Y. (2019). Development of novel 3D scaffolds using BioExtruder by the incorporation of silica into polycaprolactone matrix for bone tissue engineering. *Mater. Today Commun.* 21, 100651. doi:10.1016/j.mtcomm.2019.100651
- Pazhouhnia, Z., Beheshtizadeh, N., Namini, M. S., and Lotfikhshahshah, N. (2022). Portable hand-held bioprinters promote *in situ* tissue regeneration. *Bioeng. Transl. Med.* 7, e10307. doi:10.1002/btm.2.10307
- Peidavosi, N., Azami, M., Beheshtizadeh, N., and Ramazani Saadatnabadi, A. (2022). Piezoelectric conductive electrospun nanocomposite PCL/Polyaniline/Barium Titanate scaffold for tissue engineering applications. *Sci. Rep.* 12 (1), 20828. doi:10.1038/s41598-022-25332-w
- Peng, W., Ren, S., Zhang, Y., Fan, R., Zhou, Y., Li, L., et al. (2021). MgO nanoparticles-incorporated PCL/Gelatin-Derived coaxial electrospinning nanocellulose membranes for periodontal tissue regeneration. *Front. Bioeng. Biotechnol.* 9, 668428. doi:10.3389/fbioe.2021.668428
- Puppi, D., Piras, A. M., Piroso, A., Sandreschi, S., and Chiellini, F. (2016a). Levofloxacin-loaded star poly (ϵ -caprolactone) scaffolds by additive manufacturing. *J. Mater. Sci. Mater. Med.* 27, 44–11. doi:10.1007/s10856-015-5658-1
- Puppi, D., Piras, A. M., Piroso, A., Sandreschi, S., and Chiellini, F. (2016b). Levofloxacin-loaded star poly (ϵ -caprolactone) scaffolds by additive manufacturing. *J. Mater. Sci. Mater. Med.* 27 (3), 44. doi:10.1007/s10856-015-5658-1
- Rabionet, M., Guerra, A. J., Puig, T., and Ciurana, J. (2018b). 3D-printed tubular scaffolds for vascular tissue engineering. *Procedia Cirp* 68, 352–357. doi:10.1016/j.procir.2017.12.094
- Rabionet, M., Polonio, E., Guerra, A., Martin, J., Puig, T., and Ciurana, J. (2018a). Design of a scaffold parameter selection system with additive manufacturing for a biomedical cell culture. *Materials* 11 (8), 1427. doi:10.3390/ma11081427
- Rahman, Z., Barakh Ali, S. F., Ozkan, T., Charoo, N. A., Reddy, I. K., and Khan, M. A. (2018). Additive manufacturing with 3D printing: Progress from bench to bedside. *AAPS J.* 20, 101–114. doi:10.1208/s12248-018-0225-6
- Raj Preeth, D., Saravanan, S., Shairam, M., Selvakumar, N., Selestin Raja, I., Dhanasekaran, A., et al. (2021). Bioactive Zinc(II) complex incorporated PCL/gelatin electrospun nanofiber enhanced bone tissue regeneration. *Eur. J. Pharm. Sci.* 160, 105768. doi:10.1016/j.ejps.2021.105768
- Reddy, N., and Yang, Y. (2008). Self-crosslinked gliadin fibers with high strength and water stability for potential medical applications. *J. Mater. Sci. Mater. Med.* 19 (5), 2055–2061. doi:10.1007/s10856-007-3294-0
- Rezania, N., Asadi-Eydivand, M., Abolfathi, N., Bonakdar, S., Mehrjoo, M., and Solati-Hashjin, M. (2022a). Three-dimensional printing of polycaprolactone/hydroxyapatite bone tissue engineering scaffolds mechanical properties and biological behavior. *J. Mater. Sci. Mater. Med.* 33 (3), 31–14. doi:10.1007/s10856-022-06653-8
- Rezania, N., Asadi-Eydivand, M., Abolfathi, N., Bonakdar, S., Mehrjoo, M., and Solati-Hashjin, M. (2022b). Three-dimensional printing of polycaprolactone/hydroxyapatite bone tissue engineering scaffolds mechanical properties and biological behavior. *J. Mater. Sci. Mater. Med.* 33 (3), 31. doi:10.1007/s10856-022-06653-8
- Rezwan, K., Chen, Q., Blaker, J., and Boccaccini, A. R. (2006). Biodegradable and bioactive porous polymer/inorganic composite scaffolds for bone tissue engineering. *Biomaterials* 27 (18), 3413–3431. doi:10.1016/j.biomaterials.2006.01.039
- Rho, J.-Y., Kuhn-Spearing, L., and Zioupos, P. (1998). Mechanical properties and the hierarchical structure of bone. *Med. Eng. Phys.* 20 (2), 92–102. doi:10.1016/s1350-4533(98)00007-1
- Roh, H.-S., Lee, C. M., Hwang, Y. H., Kook, M. S., Yang, S. W., Lee, D., et al. (2017b). Addition of MgO nanoparticles and plasma surface treatment of three-dimensional printed polycaprolactone/hydroxyapatite scaffolds for improving bone regeneration. *Mater. Sci. Eng. C* 74, 525–535. doi:10.1016/j.msec.2016.12.054

- Roh, H. S., Lee, C. M., Hwang, Y. H., Kook, M. S., Yang, S. W., Lee, D., et al. (2017a). Addition of MgO nanoparticles and plasma surface treatment of three-dimensional printed polycaprolactone/hydroxyapatite scaffolds for improving bone regeneration. *Mater. Sci. Eng. C Mater. Biol. Appl.* 74, 525–535. doi:10.1016/j.msec.2016.12.054
- Ronca, A., Ronca, S., Forte, G., and Ambrosio, L. (2021). "Synthesis of an UV-curable divinyl-fumarate poly-ε-caprolactone for stereolithography applications," in *Computer-aided tissue engineering* (Netherlands: Springer).
- Russmueller, G., Liska, R., Stampfl, J., Heller, C., Mautner, A., Macfelda, K., et al. (2015). 3D printable biophotopolymers for *in vivo* bone regeneration. *Materials* 8 (6), 3685–3700. doi:10.3390/ma8063685
- Sachlos, E., and Czernuszka, J. (2003). Making tissue engineering scaffolds work. Review: The application of solid freeform fabrication technology to the production of tissue engineering scaffolds. *Eur. Cell Mater* 5 (29), 29–40. doi:10.22203/ecm.v005a03
- Saito, N., Usui, Y., Aoki, K., Narita, N., Shimizu, M., Ogiwara, N., et al. (2008). Carbon nanotubes for biomaterials in contact with bone. *Curr. Med. Chem.* 15 (5), 523–527. doi:10.2174/092986708783503140
- Salerno, A., and Domingo, C. (2015). Pore structure properties of scaffolds constituted by aggregated microparticles of PCL and PCL-HA processed by phase separation. *J. Porous Mater.* 22 (2), 425–435. doi:10.1007/s10934-015-9911-2
- Schantz, J.-T., Brandwood, A., Huttmacher, D. W., Khor, H. L., and Bittner, K. (2005). Osteogenic differentiation of mesenchymal progenitor cells in computer designed fibrin-polymer-ceramic scaffolds manufactured by fused deposition modeling. *J. Mater. Sci. Mater. Med.* 16 (9), 807–819. doi:10.1007/s10856-005-3584-3
- Shao, J., Ma, J., Lin, L., Wang, B., Jansen, J. A., Walboomers, X. F., et al. (2019a). Three-dimensional printing of drug-loaded scaffolds for antibacterial and analgesic applications. *Tissue Eng. Part C Methods* 25 (4), 222–231. doi:10.1089/ten.tec.2018.0293
- Shao, J., Ma, J., Lin, L., Wang, B., Jansen, J. A., Walboomers, X. F., et al. (2019b). Three-dimensional printing of drug-loaded scaffolds for antibacterial and analgesic applications. *Tissue Eng. Part C Methods* 25 (4), 222–231. doi:10.1089/ten.tec.2018.0293
- Shim, J.-H., Won, J. Y., Sung, S. J., Lim, D. H., Yun, W. S., Jeon, Y. C., et al. (2015). Comparative efficacies of a 3D-printed PCL/PLGA/β-TCP membrane and a titanium membrane for guided bone regeneration in beagle dogs. *Polymers* 7 (10), 2061–2077. doi:10.3390/polym71101500
- Shim, J.-H., Yoon, M. C., Jeong, C. M., Jang, J., Jeong, S. I., Cho, D. W., et al. (2014). Efficacy of rhBMP-2 loaded PCL/PLGA/β-TCP guided bone regeneration membrane fabricated by 3D printing technology for reconstruction of calvaria defects in rabbit. *Biomed. Mater.* 9 (6), 065006. doi:10.1088/1748-6041/9/6/065006
- Świątek, M., Broż, A., Tarasiuk, J., Wroński, S., Tokarz, W., Koziel, A., et al. (2019). Carbon nanotube/iron oxide hybrid particles and their PCL-based 3D composites for potential bone regeneration. *Mater. Sci. Eng. C Mater. Biol. Appl.* 104, 109913. doi:10.1016/j.msec.2019.109913
- Tarafder, S., and Bose, S. (2014). Polycaprolactone-coated 3D printed tricalcium phosphate scaffolds for bone tissue engineering: *In vitro* alendronate release behavior and local delivery effect on *in vivo* osteogenesis. *ACS Appl. Mater. Interfaces* 6 (13), 9955–9965. doi:10.1021/am501048n
- Temple, J. P., Hutton, D. L., Hung, B. P., Huri, P. Y., Cook, C. A., Kondragunta, R., et al. (2014). Engineering anatomically shaped vascularized bone grafts with hASCs and 3D-printed PCL scaffolds. *J. Biomed. Mater. Res. Part A* 102 (12), 4317–4325. doi:10.1002/jbm.a.35107
- Teoh, S.-H., Goh, B.-T., and Lim, J. (2019). Three-dimensional printed polycaprolactone scaffolds for bone regeneration success and future perspective. *Tissue Eng. Part A* 25 (13–14), 931–935. doi:10.1089/ten.tea.2019.0102
- Thadavirul, N., Pavasant, P., and Supaphol, P. (2014). Development of polycaprolactone porous scaffolds by combining solvent casting, particulate leaching, and polymer leaching techniques for bone tissue engineering. *J. Biomed. Mater. Res. Part A* 102 (10), 3379–3392. doi:10.1002/jbm.a.35010
- Tin Goh, B., Teh, L. Y., Poon Tan, D. B., Zhang, Z., and Teoh, S. H. (2014). Novel 3D polycaprolactone scaffold for ridge preservation—a pilot randomised controlled clinical trial. *Clin. Oral Implants Res.* 26, 271–277. doi:10.1111/clr.12486
- Turnbull, G., Clarke, J., Picard, F., Riches, P., Jia, L., Han, F., et al. (2018). 3D bioactive composite scaffolds for bone tissue engineering. *Bioact. Mater.* 3 (3), 278–314. doi:10.1016/j.bioactmat.2017.10.001
- Unagolla, J. M., and Jayasuriya, A. C. (2019). Enhanced cell functions on graphene oxide incorporated 3D printed polycaprolactone scaffolds. *Mater. Sci. Eng. C* 102, 1–11. doi:10.1016/j.msec.2019.04.026
- Verma, H., and Kumar, R. D., N. T. P., E. S. S. (2014). Qualitative and quantitative analysis of bone formation in the peri-implant defects grafted with polycaprolactone (pcl) alloplast enriched with platelet rich fibrin (PRF): AC linical and radiological study. *Int. J. Dent. Med. Res| SEPT-OCT* 1 (3), 30.
- Wang, C., Huang, W., Zhou, Y., He, L., He, Z., Chen, Z., et al. (2020). 3D printing of bone tissue engineering scaffolds. *Bioact. Mater.* 5 (1), 82–91. doi:10.1016/j.bioactmat.2020.01.004
- Wang, C., Meng, C., Zhang, Z., and Zhu, Q. (2022c). 3D printing of polycaprolactone/bioactive glass composite scaffolds for *in situ* bone repair. *Ceram. Int.* 48 (6), 7491–7499. doi:10.1016/j.ceramint.2021.11.293
- Wang, C., Zhao, Q., and Wang, M. (2017a). Cryogenic 3D printing for producing hierarchical porous and rhBMP-2-loaded Ca-P/PLLA nanocomposite scaffolds for bone tissue engineering. *Biofabrication* 9 (2), 025031. doi:10.1088/1758-5090/aa71c9
- Wang, F., Tankus, E. B., Santarella, F., Rohr, N., Sharma, N., Martin, S., et al. (2022a). Fabrication and characterization of PCL/HA filament as a 3D printing material using thermal extrusion technology for bone tissue engineering. *Polymers* 14 (4), 669. doi:10.3390/polym14040669
- Wang, J., Ma, X. Y., Feng, Y. F., Ma, Z. S., Ma, T. C., Zhang, Y., et al. (2017c). Magnesium ions promote the biological behaviour of rat calvarial osteoblasts by activating the PI3K/akt signalling pathway. *Biol. Trace Elem. Res.* 179 (2), 284–293. doi:10.1007/s12011-017-0948-8
- Wang, L., Kang, J., Sun, C., Li, D., Cao, Y., and Jin, Z. (2017b). Mapping porous microstructures to yield desired mechanical properties for application in 3D printed bone scaffolds and orthopaedic implants. *Mater. Des.* 133, 62–68. doi:10.1016/j.matdes.2017.07.021
- Wang, P., Wang, X., Wang, B., Li, X., Xie, Z., Chen, J., et al. (2022b). 3D printing of osteocytic Dll4 integrated with PCL for cell fate determination towards osteoblasts *in vitro*. *Bio-Design Manuf.* 5 (3), 497–511. doi:10.1007/s42242-022-00196-1
- Wang, Q., Ye, W., Ma, Z., Xie, W., Zhong, L., Wang, Y., et al. (2021). 3D printed PCL/β-TCP cross-scale scaffold with high-precision fiber for providing cell growth and forming bones in the pores. *Mater. Sci. Eng. C* 127, 112197. doi:10.1016/j.msec.2021.112197
- Wang, S., Gu, R., Wang, F., Zhao, X., Yang, F., Xu, Y., et al. (2022d). 3D-Printed PCL/Zn scaffolds for bone regeneration with a dose-dependent effect on osteogenesis and osteoclastogenesis. *Mater. Today Bio* 13, 100202. doi:10.1016/j.mtbio.2021.100202
- Wang, W., Caetano, G., Ambler, W., Blaker, J., Frade, M., Mandal, P., et al. (2016a). Enhancing the hydrophilicity and cell attachment of 3D printed PCL/graphene scaffolds for bone tissue engineering. *Materials* 9 (12), 992. doi:10.3390/ma9120992
- Wang, W., Caetano, G., Ambler, W., Blaker, J., Frade, M., Mandal, P., et al. (2016b). Enhancing the hydrophilicity and cell attachment of 3D printed PCL/graphene scaffolds for bone tissue engineering. *Mater. (Basel)* 9 (12), 992. doi:10.3390/ma9120992
- Weselucha-Birczyńska, A., Kołodziej, A., Świątek, M., Skalniak, Ł., Długoń, E., Pajda, M., et al. (2021). Early recognition of the PCL/fibrous carbon nanocomposites interaction with osteoblast-like cells by Raman spectroscopy. *Nanomater. (Basel)* 11 (11), 2890. doi:10.3390/nano11112890
- Wibowo, A., Vyas, C., Cooper, G., Qulub, F., Suratman, R., Mahyuddin, A. I., et al. (2020). 3D printing of polycaprolactone-polyaniline electroactive scaffolds for bone tissue engineering. *Materials* 13 (3), 512. doi:10.3390/ma13030512
- Williams, J. M., Adewunmi, A., Schek, R. M., Flanagan, C. L., Krebsbach, P. H., Feinberg, S. E., et al. (2005). Bone tissue engineering using polycaprolactone scaffolds fabricated via selective laser sintering. *Biomaterials* 26 (23), 4817–4827. doi:10.1016/j.biomaterials.2004.11.057
- Won, J., Park, C. Y., Bae, J. H., Ahn, G., Kim, C., Lim, D. H., et al. (2016). Evaluation of 3D printed PCL/PLGA/β-TCP versus collagen membranes for guided bone regeneration in a beagle implant model. *Biomed. Mater.* 11 (5), 055013. doi:10.1088/1748-6041/11/5/055013
- Wubneh, A., Tsekoura, E. K., Ayranci, C., and Uludağ, H. (2018). Current state of fabrication technologies and materials for bone tissue engineering. *Acta Biomater.* 80, 1–30. doi:10.1016/j.actbio.2018.09.031
- Xiao, L., Wu, M., Yan, F., Xie, Y., Liu, Z., Huang, H., et al. (2021). A radial 3D polycaprolactone nanofiber scaffold modified by biomimetic mineralization and silk fibroin coating promote bone regeneration *in vivo*. *Int. J. Biol. Macromol.* 172, 19–29. doi:10.1016/j.ijbiomac.2021.01.036
- Xie, C., Gao, Q., Wang, P., Shao, L., Yuan, H., Fu, J., et al. (2019). Structure-induced cell growth by 3D printing of heterogeneous scaffolds with ultrafine fibers. *Mater. Des.* 181, 108092. doi:10.1016/j.matdes.2019.108092
- Xu, N., Ye, X., Wei, D., Zhong, J., Chen, Y., Xu, G., et al. (2014). 3D artificial bones for bone repair prepared by computed tomography-guided fused deposition modeling for bone repair. *ACS Appl. Mater. Interfaces* 6 (17), 14952–14963. doi:10.1021/am502716t
- Xu, T., Yao, Q., Miszuk, J. M., Sanyour, H. J., Hong, Z., Sun, H., et al. (2018). Tailoring weight ratio of PCL/PLA in electrospun three-dimensional nanofibrous scaffolds and the effect on osteogenic differentiation of stem cells. *Colloids Surf. B Biointerfaces* 171, 31–39. doi:10.1016/j.colsurfb.2018.07.004
- Xu, X., Xiao, L., Xu, Y., Zhuo, J., Yang, X., Li, L., et al. (2021b). Vascularized bone regeneration accelerated by 3D-printed nanosilicate-functionalized polycaprolactone scaffold. *Regen. Biomater.* 8 (6), rbab061. doi:10.1093/rb/rbab061
- Xu, Z., Omar, A. M., and Bartolo, P. (2021a). Experimental and numerical simulations of 3D-printed Polycaprolactone scaffolds for bone tissue engineering applications. *Materials* 14 (13), 3546. doi:10.3390/ma14133546

- Xue, J., Li, X., Li, Q., Lyu, J., Wang, W., Zhuang, L., et al. (2020). Magnetic drug-loaded osteoinductive Fe₃O₄/CaCO₃ hybrid microspheres system: Efficient for sustained release of antibiotics. *J. Phys. D Appl. Phys.* 53 (24), 245401. doi:10.1088/1361-6463/ab7bb2
- Xue, R., Qian, Y., Li, L., Yao, G., Yang, L., and Sun, Y. (2017). Polycaprolactone nanofiber scaffold enhances the osteogenic differentiation potency of various human tissue-derived mesenchymal stem cells. *Stem Cell Res. Ther.* 8 (1), 148–149. doi:10.1186/s13287-017-0588-0
- Yang, X., Wang, Y., Zhou, Y., Chen, J., and Wan, Q. (2021). The application of polycaprolactone in three-dimensional printing scaffolds for bone tissue engineering. *Polymers* 13 (16), 2754. doi:10.3390/polym13162754
- Yu, Y.-Z., Zheng, L. L., Chen, H. P., Chen, W. H., and Hu, Q. X. (2014). Fabrication of hierarchical polycaprolactone/gel scaffolds via combined 3D bioprinting and electrospinning for tissue engineering. *Adv. Manuf.* 2 (3), 231–238. doi:10.1007/s40436-014-0081-2
- Yun, S., Choi, D., Choi, D. J., Jin, S., Yun, W. S., Huh, J. B., et al. (2021a). Bone fracture-treatment method: Fixing 3D-printed polycaprolactone scaffolds with hydrogel type bone-derived extracellular matrix and β -tricalcium phosphate as an osteogenic promoter. *Int. J. Mol. Sci.* 22 (16), 9084. doi:10.3390/ijms22169084
- Yun, S., Choi, D., Choi, D. J., Jin, S., Yun, W. S., Huh, J. B., et al. (2021b). Bone fracture-treatment method: Fixing 3D-printed polycaprolactone scaffolds with hydrogel type bone-derived extracellular matrix and β -tricalcium phosphate as an osteogenic promoter. *Int. J. Mol. Sci.* 22 (16), 9084. doi:10.3390/ijms22169084
- Yun, W.-S., Shim, J. H., Park, K. H., Choi, D., Park, M. I., Hwang, S. H., et al. (2018). Clinical application of 3-dimensional printing technology for patients with nasal septal deformities: A multicenter study. *JAMA Otolaryngology-Head Neck Surg.* 144 (12), 1145–1152. doi:10.1001/jamaoto.2018.2054
- Zein, I., Huttmacher, D. W., Tan, K. C., and Teoh, S. H. (2002). Fused deposition modeling of novel scaffold architectures for tissue engineering applications. *Biomaterials* 23 (4), 1169–1185. doi:10.1016/s0142-9612(01)00232-0
- Zhang, J., Zhao, S., Zhu, M., Zhu, Y., Zhang, Y., Liu, Z., et al. (2014b). 3D-printed magnetic Fe₃O₄/MBG/PCL composite scaffolds with multifunctionality of bone regeneration, local anticancer drug delivery and hyperthermia. *J. Mater. Chem. B* 2 (43), 7583–7595. doi:10.1039/c4tb01063a
- Zhang, J., Zhao, S., Zhu, M., Zhu, Y., Zhang, Y., Liu, Z., et al. (2014a). 3D-printed magnetic Fe₃O₄/MBG/PCL composite scaffolds with multifunctionality of bone regeneration, local anticancer drug delivery and hyperthermia. *J. Mater. Chem. B* 2 (43), 7583–7595. doi:10.1039/c4tb01063a
- Zhang, W., Shi, W., Wu, S., Kuss, M., Jiang, X., Untrauer, J. B., et al. (2020). 3D printed composite scaffolds with dual small molecule delivery for mandibular bone regeneration. *Biofabrication* 12 (3), 035020. doi:10.1088/1758-5090/ab906e
- Zhang, Y., Yu, W., Ba, Z., Cui, S., Wei, J., and Li, H. (2018a). 3D-printed scaffolds of mesoporous bioglass/gliadin/polycaprolactone ternary composite for enhancement of compressive strength, degradability, cell responses and new bone tissue ingrowth. *Int. J. Nanomedicine* 13, 5433–5447. doi:10.2147/ijn.s164869
- Zhang, Y., Yu, W., Ba, Z., Cui, S., Wei, J., and Li, H. (2018b). 3D-printed scaffolds of mesoporous bioglass/gliadin/polycaprolactone ternary composite for enhancement of compressive strength, degradability, cell responses and new bone tissue ingrowth. *Int. J. Nanomedicine* 13, 5433–5447. doi:10.2147/ijn.s164869
- Zhao, D., Yu, M., Lawrence, L., Claudio, P. P., B. Day, J., et al. (2020b). "Investigation of the influence of consequential design parameters on the mechanical performance of biodegradable bone scaffolds, fabricated using pneumatic micro-extrusion additive manufacturing process," in *International manufacturing science and engineering conference* (America: American Society of Mechanical Engineers).
- Zhao, S., Xie, K., Guo, Y., Tan, J., Wu, J., Yang, Y., et al. (2020a). Fabrication and biological activity of 3D-printed polycaprolactone/magnesium porous scaffolds for critical size bone defect repair. *ACS Biomaterials Sci. Eng.* 6 (9), 5120–5131. doi:10.1021/acsbmaterials.9b01911
- Zhao, S., Xie, K., Guo, Y., Tan, J., Wu, J., Yang, Y., et al. (2020c). Fabrication and biological activity of 3D-printed polycaprolactone/magnesium porous scaffolds for critical size bone defect repair. *ACS Biomater. Sci. Eng.* 6 (9), 5120–5131. doi:10.1021/acsbmaterials.9b01911
- Zimmerling, A., Yazdanpanah, Z., Cooper, D. M. L., Johnston, J. D., and Chen, X. (2021). 3D printing PCL/nHA bone scaffolds: Exploring the influence of material synthesis techniques. *Biomaterials Res.* 25 (1), 3–12. doi:10.1186/s40824-021-00204-y